PEIKKO

# WHITE PAPER

# SOIL MODULUS FOR ONSHORE WIND FOUNDATION DESIGN

Published: 11/2022 | Revised: 02/2023

# CONTENTS

# WHITE PAPER


**AUTHORS:**

**Andris Bērziņš**
Ms. Sc. Ing.
Senior Manager
Wind Energy Applications
Peikko Group Corporation

**Jānis Šliseris**
Dr. Sc. Ing.
Structural Designer
Peikko Group Corporation

**Marco D'Ignazio**
PhD
Specialist
Ramboll Finland Oy

**Ville Lehtonen**
PhD
Specialist
Ramboll Finland Oy

**Bruno di Buó**
PhD
Specialist
Ramboll Finland Oy


## 1. INTRODUCTION

**Wind turbine size and power are growing yearly, and loads on wind turbine foundations have been rapidly growing and approximately doubling in the last 8 years. Thus geotechnical design methods used in foundation design should also improve to provide an optimal foundation solution in terms of safety and cost.**

The state-of-the-art geotechnical design method is non-linear 3D soil numerical modeling with different mathematical models for different soil types and problems to solve.

The Hardening soil small strain (HSS) mathematical model is one of the best for wind turbine foundations and most soils in terms of accuracy and safety.

Any numerical soil modeling is as accurate as the geotechnical parameters selected and used in the calculations. The geotechnical parameters shall be selected accurately and fit the design problem to design a safe and cost-effective foundation model. The variability of soils often makes geotechnical design and parameter selection challenging.

The Hardening soil small strain model requires many soil parameters for each subsoil layer, and the full list is given in Table 1-1. Many parameters are well-known and easy to measure or derive from the literature, but some are less known and require more testing or research. Table 1-1 has two parts – primary and secondary. Without the primary part, the soil modeling won't be accurate enough, while the secondary part is also needed for modeling; it can be derived from the primary part and literature. Additional notes to the main parameters are given in Table 1-2.

This report presents a comprehensive study on soil modulus for different soil types, ranging from granular (sand, coarse silt, moraine) to cohesive (fine silt, clay) soils. The aim is to provide theoretical and practical guidelines for practitioners to estimate soil modulus for onshore wind turbine foundation design. The focus will be on Young's modulus $E$ and secant modulus for primary loading at 50% of the triaxial failure load $E_{50}$, secant unloading/reloading modulus $E_{ur}$, $1D$ constrained (oedometric) modulus $E_{oed}$ and initial tangent modulus at small strain $G_{max}$ or $G_0$.

The determination of soil modulus is not straightforward, as it depends, among others, on several factors, including state factors (particle density, water content, stress history, cementation) and loading factors (stresses and confinement, strain level, rate effects, number of cycles, drainage). Furthermore, an extensive set of laboratory and in-situ tests would be required to appropriately characterize soil layers across a site.

Multi-layer non-linear soil behavior can be modeled more accurately by non-linear soil material constitutive models such as hardening soil with small strain stiffness compared to linear spring models. Linear spring models cannot accurately take into account stiffness dependency on strain-stress state, backfill effect soil push-out and other important factors, that can lead to less accurate and competitive design, sometimes even wrong design that may lead to problems during wind turbine working life-time.

The study will further investigate existing correlations between measurements from in-situ methods (e.g. CPT, SPT, seismic measurements) and design parameters. Moreover, correlations between soil modulus and other laboratory geotechnical parameters will be investigated. Direct measurements of properties by oedometric or triaxial tests are omitted in this report as they are well-defined in the literature. Direct measurements are usually the best option rather than correlations.

Values of modulus for different soil types are often presented in handbooks without sufficient background information and explanation. This study aims to clarify the differences between the different modulus in the literature and provide recommendations for selecting soil modulus for Finnish soil conditions from laboratory and in-situ tests and literature.

Chapters 2 to 6 explain the theory for different deformation modulus and the factors influencing those. Chapter 7 overviews different site investigation techniques and correlations with different deformation modulus. Chapter 8 is specific to Finland, gives literature values according to NCCI 7, and is most relevant for Finnish soil conditions. And chapter 9 summarizes parameter determinations in the flowchart.

Table 1-1 Parameters for non-linear HSS model.

| Parameter | Symbol | Dimension |
|---|---|---|
| **Primary parameters** | | |
| Soil type | - | - |
| Layer thickness | - | m |
| Specific weight, no buoyancy | $\gamma_d$ | kN/m$^3$ |
| Specific weight, incl. buoyancy | $\gamma_w$ | kN/m$^3$ |
| Drained secant modulus together with reference confinement pressure | $E_{50}^{ref}$ | MPa |
| | $p^{ref}$ | kPa |
| Stiffness modulus together with reference confinement pressure | $E_{ur}^{ref}$ | MPa |
| | $p^{ref}$ | kPa |
| Critical friction angle | $\varphi$ | deg |
| Poisson's ratio | $\nu_{ur}$ | - |
| Cohesion | $c$ | kPa |
| **Secondary parameters** | | |
| Dilatancy angle | $\psi$ | deg |
| Power | $m$ | - |
| Oedometric tangent modulus, together with the reference pressure | $E_{oed}^{ref}$ | MPa |
| | $p^{ref}$ | kPa |
| $K_0$ coefficient | $K_0^{NC}$ | - |
| (if relevant) Pre-Overburden Pressure | $POP$ | kPa |
| (if relevant) Over-Consolidation Ratio | $OCR$ | - |
| Initial Young modulus or initial shear modulus at reference stress | $E_0^{ref}$ $or$ $G_0^{ref}$ | GPa |
| | $p^{ref}$ | kPa |
| Threshold shear strain | $\gamma_{0.7}$ | - |

Table 1-2 Additional notes to parameters.

| Symbol | Notes |
|---|---|
| $E_{50}^{ref}$ | EN 1997-2 specifies the secant modulus $E_{50}$. It can be measured by drained triaxial test directly or derived by methods explained in the report. |
| $E_{ur}^{ref}$ | It can be tested by triaxial test directly or derived by methods explained in the report. |
| $E_{oed}^{ref}$ | Oedometric modulus can be measured by an oedometric test or derived from methods explained in the report. |
| $c$ | In HSS modeling usually assumed 0 even for cohesive soils for drained conditions |
| $v$ | In WT foundation, HSS modeling usually assumed 0.2 even for cohesive soils |
| $\psi$ | Usually assumed 0 or friction angle minus 30 for granular soils |
| $m$ | Power exponent is usually assumed 0.4-0.5 and can be measured by triaxial testing at different confinement pressures. Not to mix with modulus number. |

# 2. SOIL MODULUS

## 2.1. Introduction

One of the major reasons for soil to deform is mechanical loading (settlement or rebound). In addition, environmental changes such as changes in water content, temperature, ground water level, and chemistry may also cause deformations. Deformations induced by loading/unloading are governed by an appropriate stress-strain curve representing the soil response to stresses.

The choice of a laboratory or in-situ test and reliable soil parameters to study a particular deformation problem in the field is not easy. Ideally, the laboratory test or the in-situ test shall aim to reproduce the deformation condition of the soil in the field at the element level or global level. For example, if the problem is a large wind turbine foundation over a comparatively thin layer of compressible soil, consolidation (oedometer) tests are often used to study the deformation behavior. Although the rigid lateral boundaries in the oedometer tes-t do not exist in the field, the confinement created by the friction between the thin clay and the stiffer top and bottom layers shall minimize the lateral displacements, well reproducing the boundary conditions within the consolidation ring. The discrepancies between laboratory and field conditions may require a correction factor in the calculations. As another example, if the problem is a shallow foundation over a deep deposit, the lateral squeezing of the soil is well represented by the horizontal deformation around, e.g., the pressuremeter; thus, the pressuremeter is well suited to predicting the settlement in such a case. In addition, the plate load test will provide information on the stiffness of the soil layers, even though the zone of influence of the test is limited to the very shallow part of the deposit because of scale effects (i.e., small diameter). These approaches also require correction factors to compensate for the lack of complete correspondence.

There are several ways to quantify the deformation characteristics of the soil. One of the simplest is through a modulus of deformation. It should be mentioned that not only soil deformation modulus affects soil deformation but also soil strength characteristics, such as size and shape of yield surface, evolution law of yield surface, flow rule of plastic deformation, etc. However, this report will be focused on the deformation modulus.

## 2.2. Modulus of deformation: general

Typical soil stress-strain curves are non-linear and depend on several factors. The initial part of that curve can be approximated by a straight line, whose slope can be related to the modulus of elasticity or Young's modulus $E$ and Poisson's ratio $v$.

Elasticity refers to the ability of a material to regain its original shape when deformed by loading. This is often not the case with soils, as they experience irrecoverable (plastic) deformations even at low stresses. Linear elasticity refers to the assumption that the stress-strain curve is linear. This concept is not fully applicable to soils, as they exhibit non-linear behavior very early in the stress-strain curve at low strain levels. Nevertheless, a constant modulus can be calculated from a stress-strain curve by using, for instance, the secant line from the origin to a given point on the stress-strain curve as in Figure 2-1 or the slope of an unload-reload cycle loop.

In the case of a triaxial test (Figure 2-1), for example, Young's modulus $E$ is given by

$$E = (\sigma_1 - \sigma_3) / \varepsilon_1 = q / \varepsilon_3 \quad (1)$$

where $\sigma_1$ and $\sigma_3$ are the major and minor principal stresses, and $\varepsilon_1 = \varepsilon_a$ (axial strain) is the major principal strain, and $q$ is deviatoric stress.

In geotechnical engineering, besides Young's modulus ($E$), shear modulus ($G$) and constrained modulus ($M$) are also defined to best define soil modulus for different applications. From the elasticity theory, the relationships for $G$ and $M$ in terms of $E$ are given as follows:

$$G = \frac{E}{2(1+v)} \quad (2)$$

$$M = E\frac{(1+v)}{(1+v)(1-2v)} \quad (3)$$

where $v$ is the Poisson's ratio.

Figure 2-1 Modulus in triaxial compression (adapted from Briaud 2013).

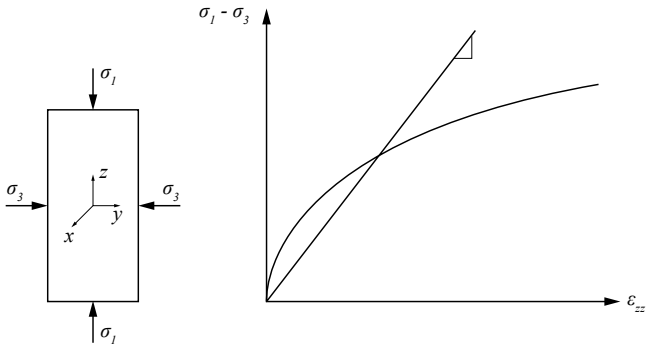

The stress-strain curve of soil, and therefore the soil modulus, is influenced by state factors and loading factors. The state factors include soil density, structure, water content, stress history, and cementation between particles. The loading factors include stress level, strain level, strain rate, number of cycles, and drainage conditions. Typically, a soil modulus increases with increasing density, decreasing water content, when the soil has been prestressed by overburden or desiccation, when cementation increases, when the mean stress level increases, when the strain level decreases, when the strain rate increases, when the number of cycles decreases, and when better drainage takes place. These aspects are discussed in Chapter 3.

## 2.3. Modulus: which one?

Due to the non-linearity of the stress-strain behavior, several modulus can be defined from a triaxial laboratory curve, for example. Figure 2-2 and Figure 2-3 show idealized deviator stress $q$ vs. axial strain $\varepsilon_a$ curve from a triaxial compression test. The deviator stress $q$ is defined as $q = \sigma_1 - \sigma_3$, where $\sigma_1$ is the major (vertical) principal stress and $\sigma_3$ is the minor (horizontal) principal stress. The value of $\sigma_3$ represents the triaxial cell pressure applied to the soil specimen. The soil modulus $E$ is defined as $E = q/\varepsilon_a$. as in Equation (1). As shown in Figure 2-2, if the modulus is drawn from the origin to a point on the curve (0 to A), the secant slope $E_s$ is obtained. One would use such a modulus for predicting, for instance, the movement due to the first load application, as in the case of a spread footing. If the slope is drawn as the tangent to the point considered on the stress-strain curve, then the tangent slope $E_t$ is obtained. One would use such a modulus to calculate the incremental movement due to an incremental load, as in the case of a movement due to one more story in a high-rise building. If the slope is drawn as the line between points A and B, then the unloading slope $E_u$ is obtained. One would use such a modulus when calculating the heave at the bottom of an excavation or the rebound of pavement after the loading by a truck tire (resilient modulus). If the slope is drawn from point B to point D, then the reloading slope $E_r$ is obtained. One would use this modulus to calculate the movement of the pavement after reloading by the same truck tire. If the slope is drawn from point B to point C, then the cyclic or unloading/reloading is obtained, and the unloading/reloading modulus $E_{ur}$ is calculated from it. The $E_{ur}$ is taken as the secant modulus representing an unloading/reloading loop. One would use such a modulus and its evolution as a function of the number of cycles to calculate the movement of a pile foundation subjected to repeated wave loading.

Ideally, a secant modulus should be determined for a stress and strain range that best reflects the actual loading conditions. Moreover, regardless of which modulus is defined and considered, the state of the soil at any given time will affect that modulus.

Figure 2-2 Definition of soil modulus $S$. For $\sigma$ (in the plot) = $q$ and $\varepsilon = \varepsilon_a$, $S = E$ (adapted from Briaud 2013).

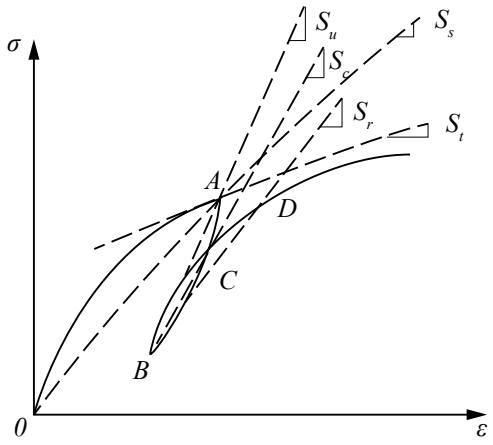


Figure 2-3 Representative stress-strain-strength curve of soil in triaxial compression mode (Rix et al. 2019).

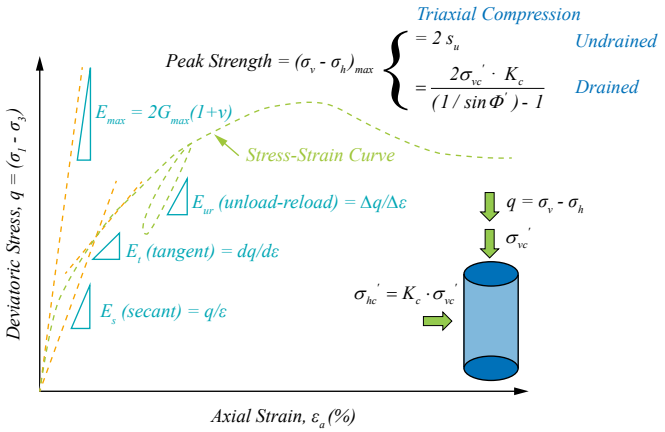

# 3. FACTORS INFLUENCING SOIL MODULUS

## 3.1. State factors

The state factors include particle packing and organization, water content, stress history, and cementation.

### 3.1.1 Particle packing and organization

If soil particles are closely packed, the modulus tends to be high. This is measured by the dry density (ratio of the weight of solids over the total volume of the wet sample) of the soil, for example, it can also be measured by the porosity (ratio of the volume of voids over the total volume of the wet sample). Besides dry density or porosity, soil structure will also affect the modulus. For example, coarse-grained soil can have a loose or dense structure; fine-grained soil can have a dispersed or flocculated structure. While two soil samples can have the same dry density, their structures and, therefore, their modulus can be significantly different. This somewhat explains with recovering a disturbed sample of coarse-grained soil in the field and reconstituting it to the same dry density and water content in the laboratory can reveal notable differences between the laboratory and field modulus. (Briaud 2013).

### 3.1.2 Water content

The water or moisture content has a major impact because, at a low degree of saturation, the water binds the particles (especially for fine-grained soils) and increases the effective stress between the particles through the water tension (suction) phenomenon. Therefore, in this case, low saturation leads to high soil modulus. This explains why clay shrinks and becomes very stiff when it dries. For fully saturated fine-grained soils (clays and silts), the modulus tends to decrease with increasing water content. In relation to coarse-grained soils (silt, sand, moraine, gravel), the compaction at a very low degree of saturation is not as efficient as it is at higher saturation because the lubrication effect of water is not present. Therefore, in this case, very low saturation leads to low modulus. As the saturation and, therefore, water content increase, water lubrication increases the effect of compaction, and the modulus increases as well. However, if the degree of saturation rises beyond an optimum value, the water occupies more and more room and gets to the point where it pushes the particles apart, thereby increasing compressibility and reducing the modulus. (Briaud 2013).

### 3.1.3 Stress history

Another major factor affecting the soil modulus is the stress history. A soil that has been preloaded in the past is called “overconsolidated”. Preloading could come, for example, from a glacier that has now totally melted, from drying and wetting cycles, or from mechanical preloading. If the soil has not been preloaded in the past, meaning that the current stress level is the highest effective stress ever experienced by the soil, the soil is “normally consolidated”. An overconsolidated ($OC$) soil will generally have higher modulus than the same normally consolidated ($NC$) soil because the $OC$ soil is on the reloading part of the stress-strain curve, whereas the $NC$ soil is on the first loading part. Some soils are still in the process of consolidating under their own weight. These so-called under-consolidated soils are characterized by the fact that the deposition rate of the sediments (e.g., in a river delta) is faster than the rate that would allow the pore water pressures induced by deposition to dissipate. These clays have very low modulus. (Briaud 2013).

### 3.1.4 Cementation

Cementation refers to the glue-like bonds that may exist at the contact surface between particles. As mentioned above, a low degree of saturation in fine-grained soils can generate water tension strong enough to simulate a significant “glue effect” between particles. Another glue effect is due to the chemical cementation that can develop at the contact. This cementation can be due to the deposition of calcium at the particle-to-particle contacts, for example. Such cementation leads to a significant increase in modulus. (Briaud 2013).

## 3.2. Loading factors

In this section, it is assumed that the state factors for the soil considered are fixed (unchanging). In other words, the discussion of each of the following factors can be prefaced by saying “all other factors being equal”. Also, in this section, the secant modulus is used.

### 3.2.1 Stresses and confinement

During a loading process, the applied loads induce stresses in the soil. These stresses can be shear stresses or normal stresses, or a combination of both. In undrained conditions, the initially generated excess pore pressure will dissipate and lead to an increase in effective stress. In drained conditions, the applied load is transferred to the soil as effective stress. At any given point and at any given time in a soil mass, there is a set of three principal normal stresses, which are generally referred to as $\sigma_1$ , $\sigma_2$ , and $\sigma_3$ . (total) $\sigma_1'$ or $\sigma_2'$, and $\sigma_3'$ (effective).

For triaxial conditions, $\sigma_2' = \sigma_3'$. The mean of these three stresses is often referred to as $\sigma_M$ or $p'$ and is defined as $\sigma_M = p' = \left(\sigma_1' + \sigma_2' + \sigma_3'\right) / 3$ .

The mean effective stress has a significant influence on the soil modulus. This can be referred to as the "confinement effect". Figure 3-1 and Figure 3-2 illustrate three ideal stress-strain curves at three different confinement pressures $\sigma_3$ . Pressure $\sigma_3$ represents the triaxial applied cell pressure at which each sample is consolidated.

As shown, the higher the confinement is, the higher the soil modulus will be. In particular, the two figures show the variation of the secant modulus for primary loading at 50% of the maximum deviator stress, known as $E_{50}$.

Figure 3-1 Triaxial compression stress-strain curves for different cell pressures and influence on secant modulus at 50% of the maximum deviator stress ($E_{50}$) (Mansikkamäki 2022).

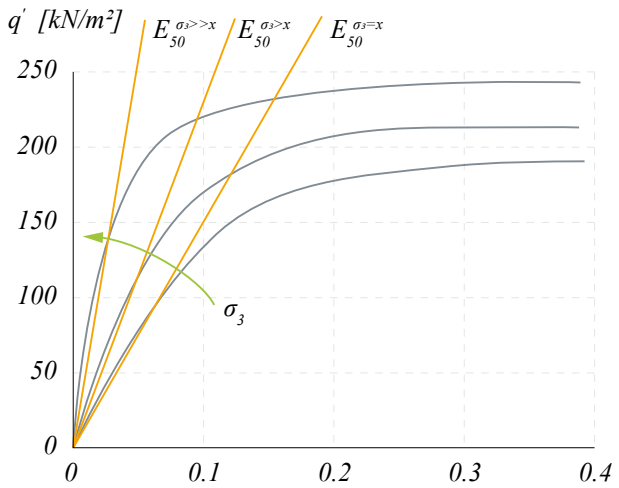


A common model for quantifying the influence of confinement on the soil modulus is given in Equation (4) and is usually attributed to the work of Kondner (1963) and Janbu (1963).

According to this model, the modulus is proportional to a power law of the confinement stress. The modulus $E_{50}^{ref}$ is the modulus obtained at confinement stress that is taken equal to the atmospheric pressure $p_a$ or reference stress $p^{ref}$ (= 100 kPa).

The exponent $\beta$ varies according to the soil type. A common $\beta$-value for granular soils is 0.5, while it is ≈0 for clays. Typical values of $E_{50}^{ref}$ are 15–50 MPa for loose to dense sands and 1–3 MPa for fairly soft, normally consolidated, or lightly overconsolidated clays. Highly $OC$ clays are stiffer.

$$E_{50} = E_{50}^{ref} \left( \frac{\sigma_3}{p^{ref}} \right)^{1-\beta} \quad (4)$$

Figure 3-2 Stress-dependent secant shear modulus $E_{50}$ from triaxial compression tests (Mansikkamäki 2022).

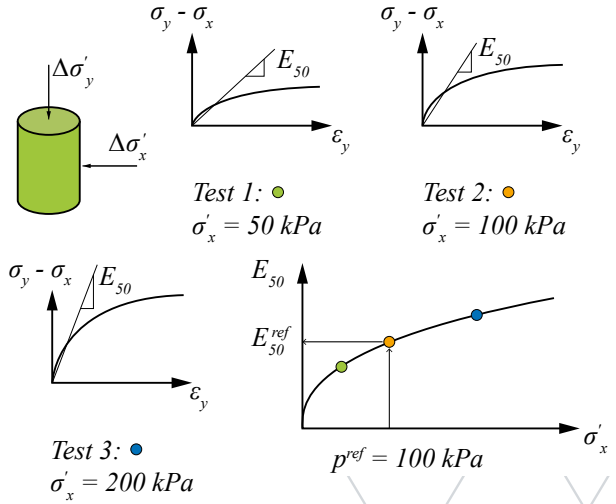

### 3.2.2 Strain level

The loading process induces strains in the soil mass. Since soils are non-linear materials, the secant modulus depends on the strain levels in the zone of influence. In general, the secant modulus will decrease as the shear strain level increases due to an increase in shear stress mobilization. This is due to the downward curvature of the stress-strain curve.

An exception to this downward curvature occurs when the results of an oedometer consolidation test are plotted as a stress-strain curve on arithmetic scales for both axes. In this case, the stress-strain curve is characterized by an upward curvature. This is explained by the fact that the deviatoric stress mobilization level stays constant due to the lateral constraint, and volumetric strains cause a reduction in pore space, resulting in a stiffer soil structure.

In a triaxial test, the resulting stress-strain curve can be fitted with a hyperbolic model up to the peak value; the associated model for this modulus is shown in Figure 3-3 and Equation (5). (Duncan and Chang 1970). In this model, $E_0$ is the initial tangent modulus, also equal to the secant modulus for a strain of zero.

The parameter $s$ the asymptotic value of the stress for an infinite value of strain and is related to the strength of the soil.

$$E = \left( \frac{1}{E_0} + \frac{\varepsilon}{s} \right)^{-1} \quad (5)$$

Figure 3-3 Impact of strain level on soil modulus (Briaud 2013).

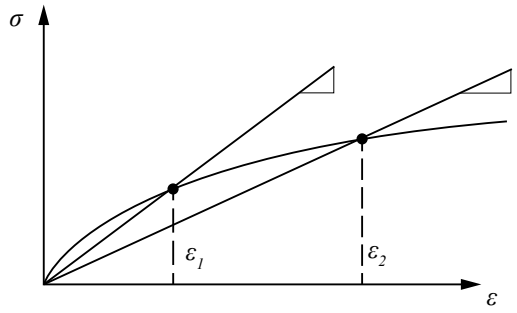


### 3.2.3 Rate dependency

Soils are viscous materials, meaning that the faster a soil is loaded, the stiffer its response is. In some cases, though, the reverse behavior is observed. This effect can occur even without significant drainage.

Figure 3-4 shows an example of two stress-strain curves obtained by loading the soil at two different strain rates.
Strain rate is defined as the strain accumulated per unit of time. The modulus usually varies as a straight line on a log-log plot of modulus vs. strain rate.

The slope of that line is represented by the exponent $b$ in Equation (6). In clays, common values of this exponent vary from 0.02 for stiff clays to 0.1 for very soft clays. In sands, common values of b vary from 0.01 to 0.03.

The $b$ values suggest strain rate to be more significant in fine-grained soils, while for coarse-grained soils, the effect of strain rate is normally neglected in practice.

$$E = E_0 \left( \frac{\dot{\varepsilon}_2}{\dot{\varepsilon}_1} \right)^b \quad (6)$$

Figure 3-4 Impact of strain rate on soil modulus (Briaud 2013).

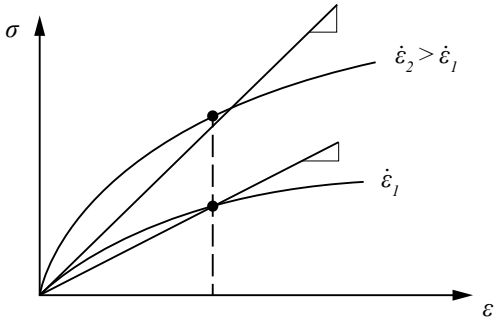

### 3.2.4 Number of cycles

If the loading process is repeated several times cyclically, the number of cycles applied will influence the soil modulus. With reference to the secant modulus, the larger the number of cycles, the smaller the modulus becomes (Figure 3-5).

This is consistent with the accumulation of strain with an increasing number of cycles. A model that can be used to describe this phenomenon is presented in Equation (7).

The exponent $c$ in the model is negative and varies significantly. The most common values are on the order of -0.1 to -0.3.

Nevertheless, it is recommended to run cyclic soil tests to evaluate the coefficient $c$, as cyclic response varies significantly along with soil properties and cyclic amplitudes.

$$E = E_0 N^{-c} \tag{7}$$

Figure 3-5 Impact of number of cycles on soil modulus (Briaud 2013).

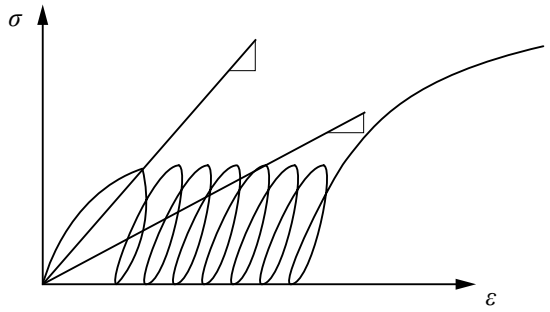


### 3.2.5 Drainage

Drainage during loading will affect the soil response and, therefore, the soil modulus. In general, one can refer to two extreme cases that can occur: drained or undrained loading. The undrained case may occur if the drainage valve is closed during a laboratory test or if the test is run sufficiently quickly in the field.

The time required to maintain an undrained behavior or to ensure complete drainage depends mainly on the soil type (permeability) and the length of the drainage path. For example, a 10-minute test in high-plasticity clay is probably undrained, whereas a 10-minute test in clean sand is probably drained.

The Poisson's ratio is also sensitive to drainage. For example, if no drainage takes place during loading in clay, it is common to assume a Poisson's ratio $\nu_u$ equal to 0.5 (no volume change).

In contrast, if complete drainage takes place (excess pore pressure is kept equal to zero), then Poisson's ratio values of 0.2 – 0.35 ($\nu$) may be reasonable. It must be noted that the shear modulus $G$ remains theoretically constant and does not vary with drainage. This is because the effective shear stress is equal to the total shear stress.

Note also that the Poisson's ratio can be larger than 0.5 if the soil dilates during shear associated with compression.

# 4. INITIAL (SMALL-STRAIN) TANGENT MODULUS

The initial shear modulus reflects small strain conditions and is, therefore, representative of situations where the applied load is only a small fraction of the foundation failure load. For instance, dynamic (seismic) calculations shall be checked using a modulus value compatible with small loads and strains (e.g., for earthquake or railroad vibration calculations). Actually, it is more accurate to always calculate with a small strain stiffness procedure, and the software should use small strain stiffness in small strain regions, and in regions with larger strains, use smaller stiffness.

This modulus is typically referred to as $G_0$ or $G_{max}$. This is because the shear modulus $G$ is more convenient than Young's modulus $E$. Indeed, the shear modulus $G$ does not require knowledge of Poisson's ratio, whereas $E$ does.

The subscript "*0*" or "*max*" refers to the fact that it is the modulus at the origin and also the maximum shear modulus value one can expect for the soil. Several expressions for $G_{max}$ have been formulated. Hardin and Drnevich (1972) and Hardin (1978) proposed, for all soil types:

$$\frac{G_{max}}{p_a} = \frac{625}{0.3+0.7e^2}(OCR)^k \left(\frac{p'}{p_a}\right)^n \qquad (8)$$

where $p_a$ is the atmospheric pressure, $e$ is the void ratio, $OCR$ is the over-consolidation ratio, $p'$ is the mean effective normal stress ($p'=(\sigma_1+\sigma_2+\sigma_3)/3$), and $k$ and $n$ are exponents.

The exponent $n$ is usually taken equal to 0.5, and $k$ varies with the plasticity index ($k$ = 0.00, 0.18, 0.30, 0.41, 0.48, 0.50 for $I_p$ = 0, 20, 40, 60, 80, 100).

Figure 4-1 Initial shear modulus $G_0$ as a function of void ratio (after Benz 2007).

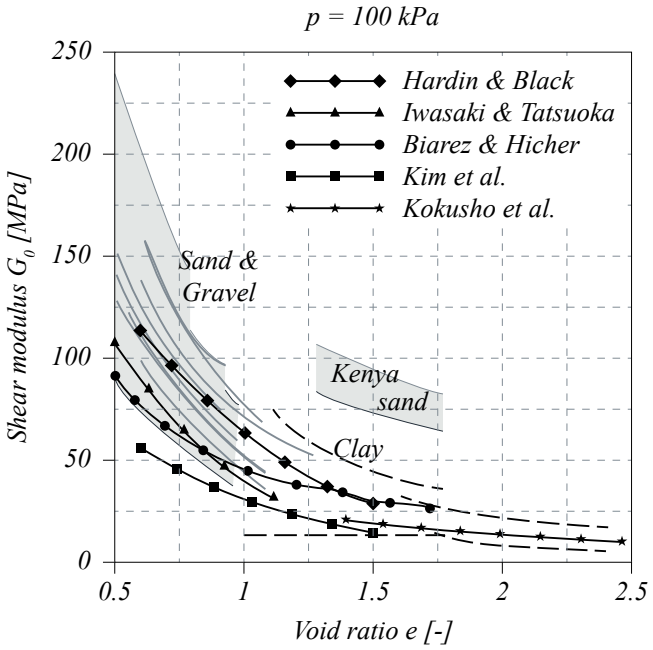

For fine-grained soils, Andersen (2015) proposed a relationship between $G_{max}$ and the undrained shear strength $s_u$ measured in direct simple shear tests (note that this is roughly comparable to $s_u$ determined by field vane testing) as a function of the plasticity index ($I_p$; in %) and the $OCR$. The relationship is described by Equation (9) and illustrated in Figure 4-2.

$$G_{max}s_{uD} = \left(30 + \frac{300}{I_p / 100 + 0.03}\right) OCR^{-0.25} \qquad (9)$$

Figure 4-2 Initial shear modulus $G_{max}$ normalized by undrained shear strength from direct simple shear tests ( $s_u^{DSS}$ ) as a function of $OCR$ and $I_p$ (Andersen 2015).

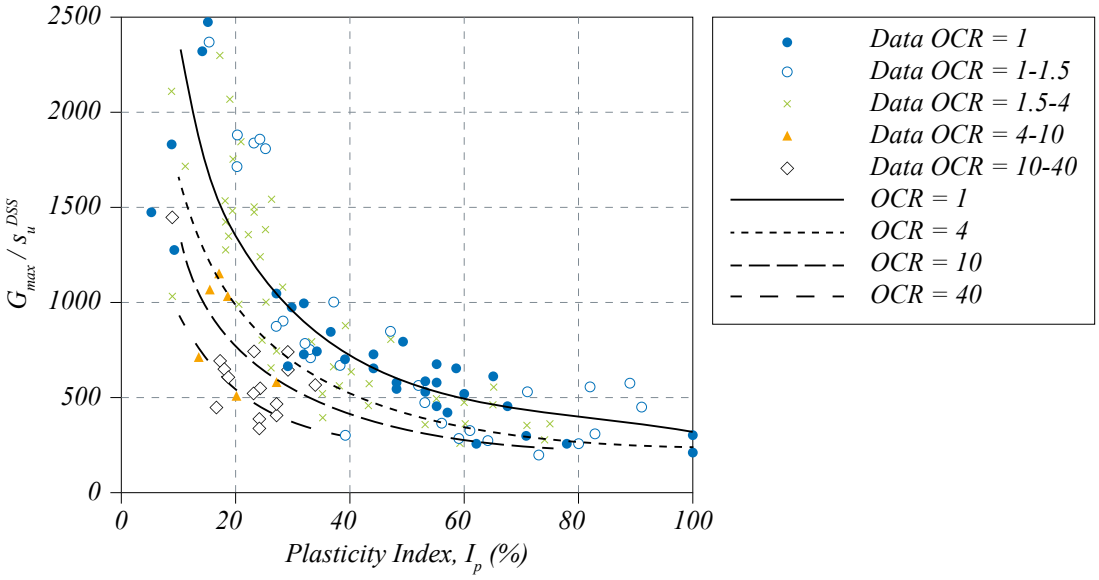


In the end, however, testing is the best way to obtain $G_{max}$. In the field, the tests that can be used are, among others, the cross-hole test and the seismic CPTu. In the laboratory, the best test is the resonant column test, yet sample disturbance may lead to lower values of $G_{max}$ compared to the field values. The field values come from testing a large, undisturbed mass of soil through wave propagation, whereas disturbance has a much more pronounced effect on the small scale of the lab test. The contrary is likely true for weathered rocks, where the sample is likely to be much stiffer than the rock mass (Briaud 2013).

The $G_{max}$ is linked to the shear wave velocity by the elasticity theory as:

$$G_{max} = pV_s^2 \qquad (10)$$

Where $G_{max}$ is the shear modulus (in $p_a$), $V_s$ is the shear wave velocity (in m/s), and $p$ is the density (in kg/m$^3$).

$$E_{max} = 2G_{max}(1+\nu) \qquad (11)$$

The values of $G_{max}$ ($G_0$) or $E_{max}$ ($E_0$) can be obtained from undisturbed samples in the laboratory using a resonant column test, bender elements, or special triaxial apparatus outfitted with local strain measurements. Better yet, in-situ tests are more reliable because they are unaffected by sample disturbance, stress relief, and small specimen size effects.

It is suggested that for Poisson's ratio in Eq. 11, $\nu \approx \nu_{ur}$ = 0.2 is used.

Typical Poisson's ratio values for drained conditions range between 0.2 and 0.35 for a wide range of soils (e.g., Briaud 2013).

In undrained conditions, $\nu \approx 0.4–0.5$. A value of $\nu_u = 0.5$ corresponds to constant volume deformation as assumed in undrained conditions. Lower $\nu$ values (< 0.15) are observed for very loose sands and very soft clays (Briaud 2013) or generally at very small strains.

Figure 4-3 shows the evolution of Poisson's ratio as a function of strain in a drained triaxial test on an overconsolidated clay specimen. Values of $\nu < 0.10$ are observed at $\varepsilon_a < 10^{-4}$, reaching a steady value already around $\varepsilon_a \approx 10^{-3}$. For onshore wind gravity-based foundations, the strains reached during primary loading are generally > $10^{-3}$ (0.1%), suggesting the use of $\nu > 0.1$.

A Poisson's ratio of 0.1 may be used at very small strains to determine e.g. $E_{max}$ from Equation (12).

Figure 4-3 Incremental Poisson's ratio from drained triaxial compression test on overconsolidated clay (Länsivaara 1999).

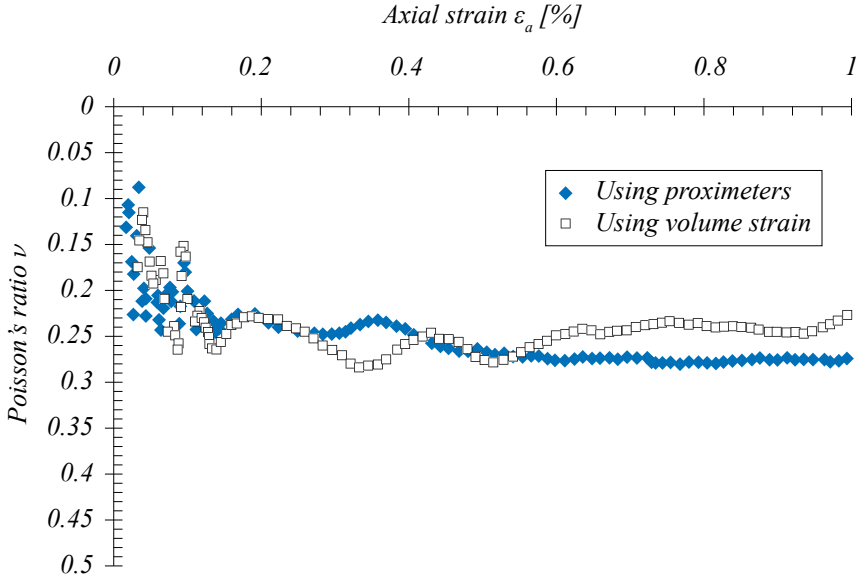


The initial tangent shear and Young's modulus can be used directly when strains are small $\varepsilon < 10^{-6}$ (e.g., dynamically loaded foundations, site amplification for low-intensity ground motions); however, in many cases, a modulus reduction factor (MRF) must be used to adjust the value of shear or Young's modulus to the appropriate level of strain ($\varepsilon$ or $\gamma$) or mobilized stress ($q/q_{max}$ or $\tau/\tau_{max}$). For cyclic loading, the use of resonant column tests can be used to obtain the shear modulus reduction curve.

For monotonic (i.e., static) loading, torsional shear tests and special triaxial tests with local strain sensors provide the MRF curves for each soil. For empirical estimates, MRF values for cyclic loading may be found from well-known modulus reduction relationships (e.g., Vucetic and Dobry 1991, Darendeli 2001). A recent method for MRF curves for both monotonic and cyclic loading of clays is presented by Vardanega and Bolton (2013).

For first-time monotonic loading of soils, the MRF trend in Figure 4-4 is shown in terms of mobilized stress, which is the reciprocal of the safety factor: 1/FS = $q/q_{max} = \tau/\tau_{max}$. The data are derived from undrained and drained resonant column-torsional shear tests and specially instrumented triaxial tests conducted on sands and clays. An algorithm that expresses the trend is given by the following:

$$MRF = 1-\left(q / q_{max}\right)^g = 1-\left(\tau / \tau_{max}\right)^g = 1-\left(1 / FS\right)^g \qquad (12)$$

where
$g$ = fitting parameter

For an initial estimate, the exponent $g$ generally takes a value of approximately 0.3 for uncemented sands and inorganic clays of low sensitivity. Thus, the relevant value of $G$ (similarly for $E$) for a particular problem can be obtained from the following:

$$G = MRF \; G_{max} \tag{13}$$

For instance, at 50% of $\tau_{max}$, assuming $g$ = 0.3, $G_{50}$ = 0.19 $G_{max}$.

Figure 4-4 Modulus reduction factor of sands and clays in drained and undrained loading expressed in terms of mobilized strength (Mayne 2007).

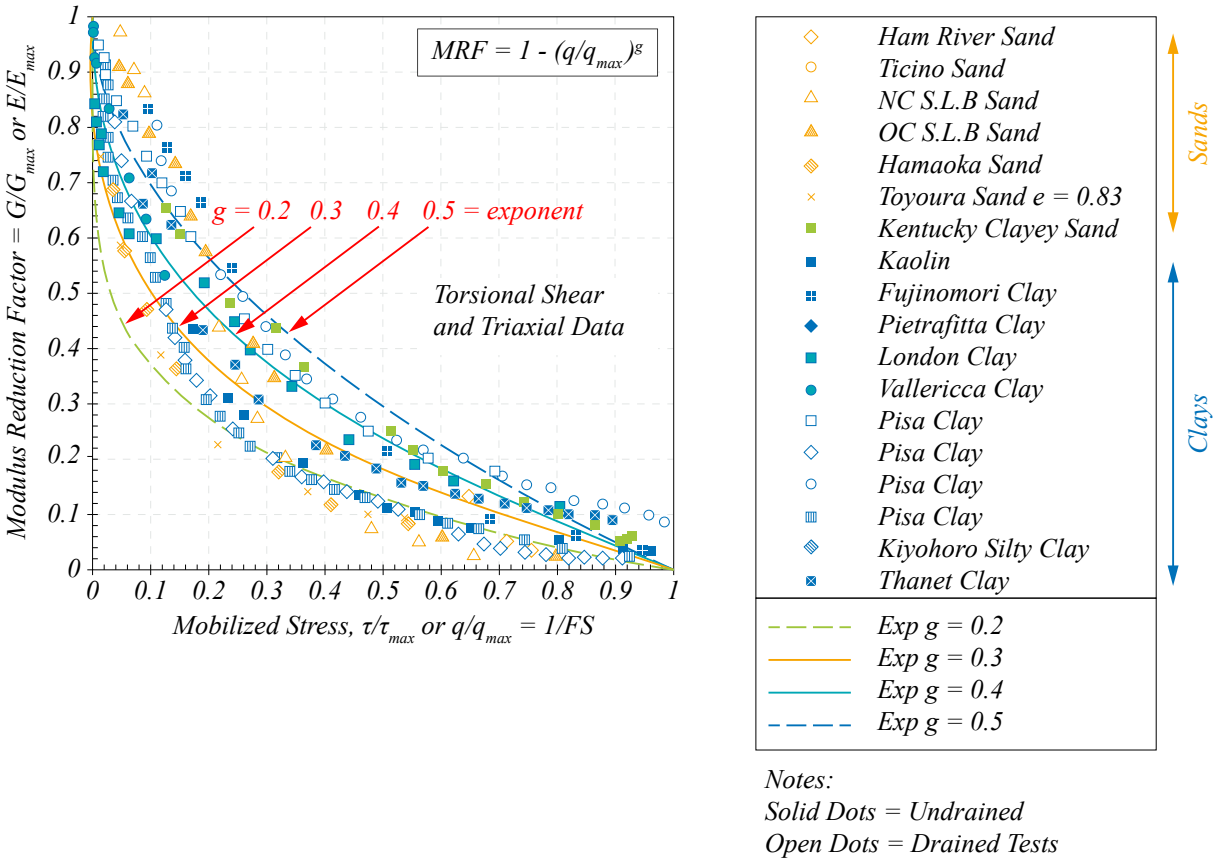

# 5. UNLOADING/RELOADING MODULUS

Figure 5-1 illustrates how the unloading/reloading modulus $E_{ur}$ is not constant and varies according to the amplitude of the unloading/reloading cycles and strain level. It should be mentioned that $E_{ur}$ is used not only in unloading-reloading cycles but is used more generally in the HSS model to calculate elastic strains. Therefore, this parameter affects and governs the soil's elastic part and will affect it results even if there are no unloading/reloading cycles.

While triaxial test data are ideal for obtaining $E_{ur}$, in-situ tests such as the pressuremeter test are known to provide unloading/reloading modulus. However, the pressuremeter test is not used in Finland, while tests such as plate load test and falling weight deflectometer are used in road constructions. In the absence of laboratory data, $E_{ur}$ can be estimated based on Figure 5-2, based on the empirical relation proposed by Alpan (1970). The relation relates the so-called "static" modulus $E_s$ to the "dynamic" modulus $E_d$. The static modulus can be considered as $E_{ur}$ obtained at engineering strain levels ($\varepsilon \approx 10^{-3}$), whereas $E_0$ can be considered as $\approx E_d$, corresponding to the initial or small-strain modulus defined in the previous section (Alpan 1970, via Obrzud and Truty 2018).

Figure 5-1 Definition of unloading-reloading modulus from triaxial compression test (Mansikkamäki, 2022).

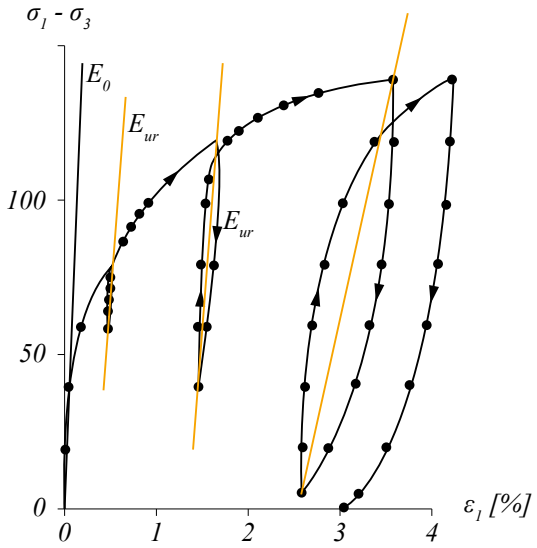


Figure 5-2 Approximative relation between" static" soil modulus (here $E_s \approx E_{ur}$) and" dynamic" modulus $E_d$ corresponding to $E_0$ proposed by Alpan (1970).

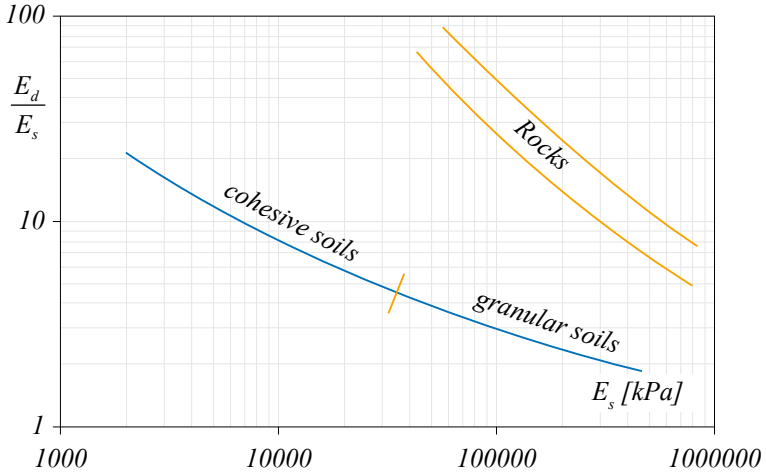

Typically, when $E_{50}$ or $E_{ur}$ cannot be directly determined from experimental curves, it may be relevant for many practical cases to assume (Obrzud and Truty 2018):

$$\frac{E_{ur}}{E_{50}} = 2 \text{ to } 6 \qquad (14)$$

Higher ratios can be assumed for loose sands (3 to 6) or clays (5 to 10), whereas lower for dense sands (2 to 4) or crushed aggregates (≈ 2). Well-compacted aggregates typically exhibit even lower ratios. The compaction has, however, resulted in an "overconsolidated" soil state, so any subsequent loading may actually be considered a reloading event.

# 6. CONSTRAINED OEDOMETER MODULUS

## 6.1. Soil behavior in one-dimensional compression

For a non-linear response, like in most soils, the resistance to action is generally defined as the tangent of the action-response curve. The tangent value will, therefore, vary with the action (Janbu 1998).

Figure 6-1 shows four different stress-strain relationships from 1D oedometer consolidation tests, all in arithmetic scale. The stress $\sigma'$ represents the vertical effective stress $\sigma'_v$ or $\sigma'_1$. The diagrams represent:

a) an overconsolidated clay, where $\sigma'_c > \sigma'_{v0}$ *(OC)*
b) silty sand at in situ porosity, approximately normally consolidated (*NC*)
c) an intact sample of a cemented moraine, a shale, or a sedimentary rock
d) a sample of intact, fairly undisturbed, sensitive clay with a loose, porous structure, easily collapsible for increasing $\sigma'$ around $\sigma'_c$.

Figure 6-1 Typical stress-strain curves from oedometer tests. Arithmetic plots (Janbu 1998).

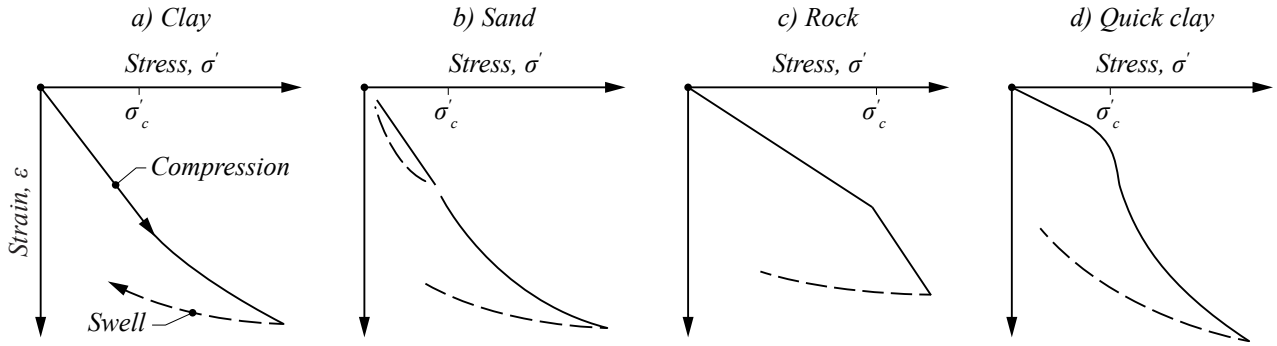


Figure 6-2 Typical $M - \sigma'$ relationships from $\sigma' - \varepsilon$ curves obtained by oedometer tests (Janbu 1998).

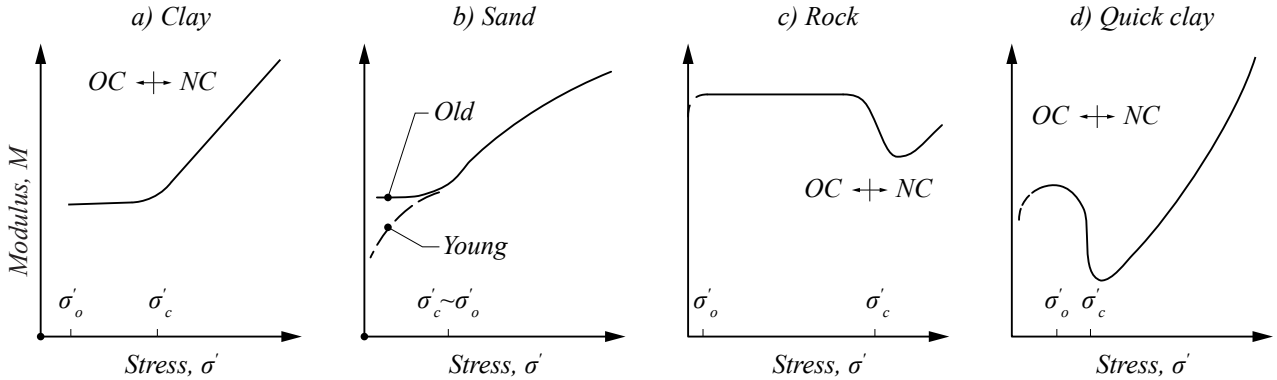

The value of the tangent modulus M is plotted in Figure 6-2 as a function of the effective stress $\sigma'$. All four diagrams show that $M$ depends on $\sigma'$. In particular, the $M-\sigma'$ variation appears to change character around a certain stress range, denoted $\sigma'_c$ = pre-consolidation pressure. Consequently, there is one trend of behavior for $\sigma' < \sigma'_c$ (the $OC$ range) and a different trend for $\sigma' > \sigma'_c$ (the $NC$ range).

The change of the $M-\sigma'$ pattern is most dramatic for sample (*d*) in Figure 6-2, representing the sensitive or extra-sensitive soil. For $\sigma' < \sigma'_c$, the $M_{OC}$-value is fairly constant and relatively high. When $\sigma'$ just passes $\sigma'_c$, the $M$-value drops dramatically to approximately 20% of $M_{OC}$. Given that $M$ is primarily caused by an internal shearing resistance within the grain structure, this implies that the grain structure loses most of its internal resistance when $\sigma' > \sigma'_c$. In other words, the grain structure collapses (at least partly) and/or loses most of its internal rigidity due to the breakage of contact points between mineral grains. These "cemented" particle contacts have been established over geological time periods (Janbu 1998).

Figure 6-1 and Figure 6-2 indicate that $\sigma'_c$ shows up as a change in the shape of the arithmetic curves ($\sigma' - \varepsilon$) and ($M-\sigma'$).

## 6.2. Tangent constrained modulus formulation

In practical engineering, it is possible to use one simple formula for $M = f(\sigma')$ to cover all the variations indicated in Figure 6-2. The idealized formula is:

$$M = mp^{ref}\left(\frac{\sigma'}{p^{ref}}\right)^{1-\beta} \qquad (15)$$

where:
$M$ = tangent modulus (kPa, MPa)
$p^{ref}$ = reference stress = 100 kPa ≈ 1 atm
$\sigma'$ = intergranular pressure, i.e. effective vertical stress (kPa, MPa)
$m$ = modulus number (dimensionless)
$\beta$ = stress exponent (dimensionless)

The four main categories of $M-\sigma'$ variations can be described by this one generalized formula, exemplified by four $\beta$-variations, namely:

- $M = mp^{ref} = M_{OC}$ = constant for $\beta$ = 1, corresponding to overconsolidated soil ($\sigma' > \sigma'_c$) denoted $OCS$ or $EE$ (equivalent elastic)
- $M = m\left(\sigma' \cdot p^{ref}\right)^{0.5}$ for $\beta$ = 0.5, corresponding to normally consolidated sand, denoted $NCS$, for $\sigma' > \sigma'_c$. In silty sandy soils (NC), the $\beta$-value may typically range between 0.4 to 0.65, so $\beta$ = 0.5 should be considered an average choice for practical purposes only.
- $M = m\sigma'$ for $\beta$ = 0 corresponding to normally consolidated clays, $NCC$. Here, the meaning of the modulus number is very clear, as the slope of the $M-\sigma'$ line is equal to $m$.
- $M = m\sigma'\left(\sigma' \; p^{ref}\right)^{0.5}$ for $\beta$ = -0.5, corresponding to normally consolidated extra-sensitive clays, $NCES$. For Scandinavian sensitive clays, the $\beta$-value may range from -0.3 to -0.5.

Figure 6-3 shows how a variable $\beta$ from -0.5 to +1 can cover all mineral soils from rock to very porous and extra soft soils. Generally, $\beta$ decreases as the porosity of the granular medium increases.

Figure 6-4 shows clearly that it is the modulus number, $m$, that gives the order of magnitude of the modulus $M$. The $m$-value ranges from a low of $m$ = 2 to 5 for $n$ ≈ 80% to 90%, via $m$ = 10 to 100 for $n$ ≈ 50%, and further on to $m$ = 104 to 106 for $n$ = 5 to 10%.

Figure 6-3 a) Tangent modulus versus stress and b) stress exponent for a range of soils (Janbu 1998). Note that here instead of $\beta$, the letter α is used.

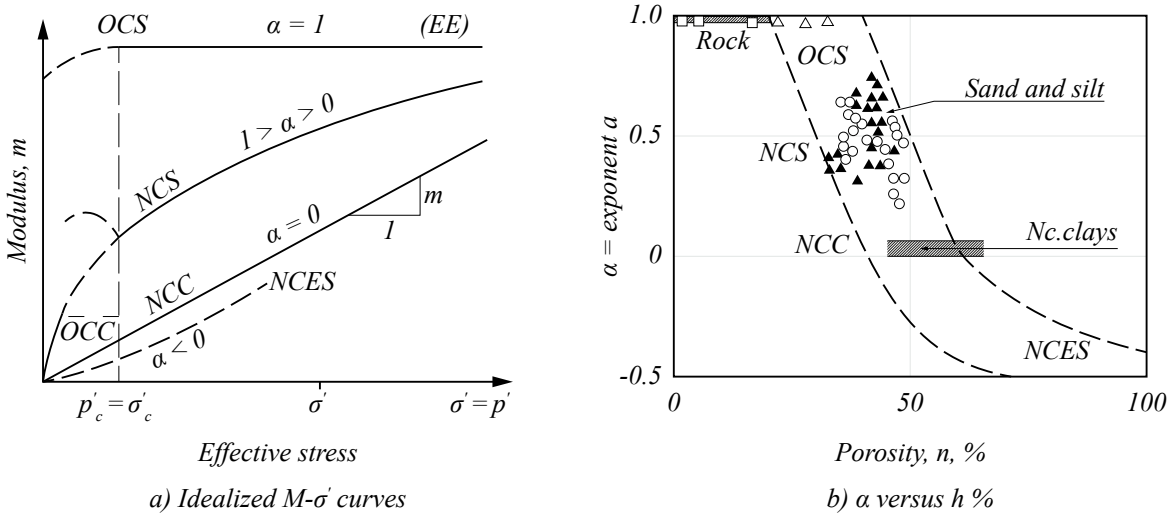


Figure 6-4 Modulus number as a function of porosity for a range of soils (Janbu 1998).

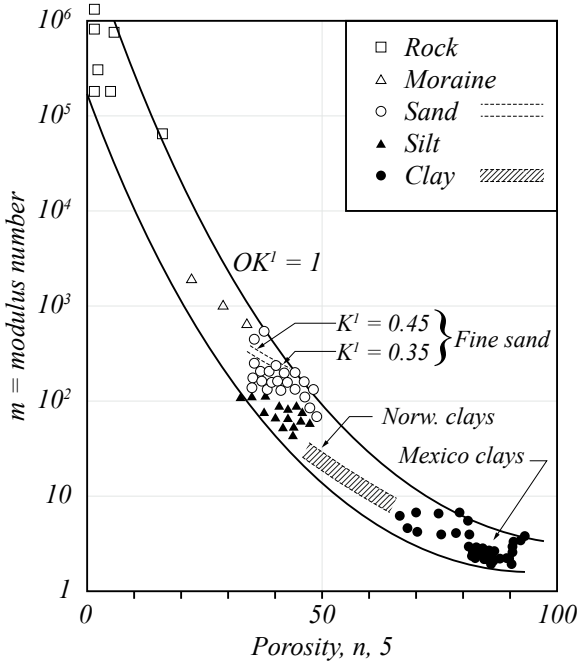


For normally consolidated clays with $\beta = 0$ and $M = m\sigma'$ $(NCC)$, $m$ = 8–25 for soft to medium clays (water content $w$ = 70–25% or porosity $n$ = 65–40%) (Janbu 1998).

For normally consolidated silty-sandy soils, with $\beta = 0.5$ and $m\left(\sigma' \cdot p^{ref}\right)^{0.5}$ (type $NCS$), typical $m$-variations for loose to dense states are found as follows:
$m$ = 50–100 (silt)
$m$ = 100–500 (sand)

For overconsolidated clays with $\beta = 1$, the generalized formula gives $M = mp^{ref}$ = constant (type $OCC$). This means that $M$ is independent of $\sigma' = \sigma'_0 + q$ when $\sigma'_c >> \sigma'_0 + q$. Experience has shown that the value of $M_{OC}$ is uniquely expressed as (Janbu 1998).

$$M_{OC} = m_c \sigma'_c$$

where $m_c = f(w)$ as in clays. Since most $OC$ clays have low water content (< 25%), it means that $m_c$ = 25–50.
For saturated clays, Janbu (1998):

$m = 700/w_n$ (uncertainty 30%) (16)

Karlsrud and Hernandez-Martinez (2013) proposed the relationships in Figure 6-6 based on high-quality samples for Norwegian sensitive clays.

Figure 6-5 Relationship between modulus number for primary (virgin) loading and natural water content (Janbu 1998).

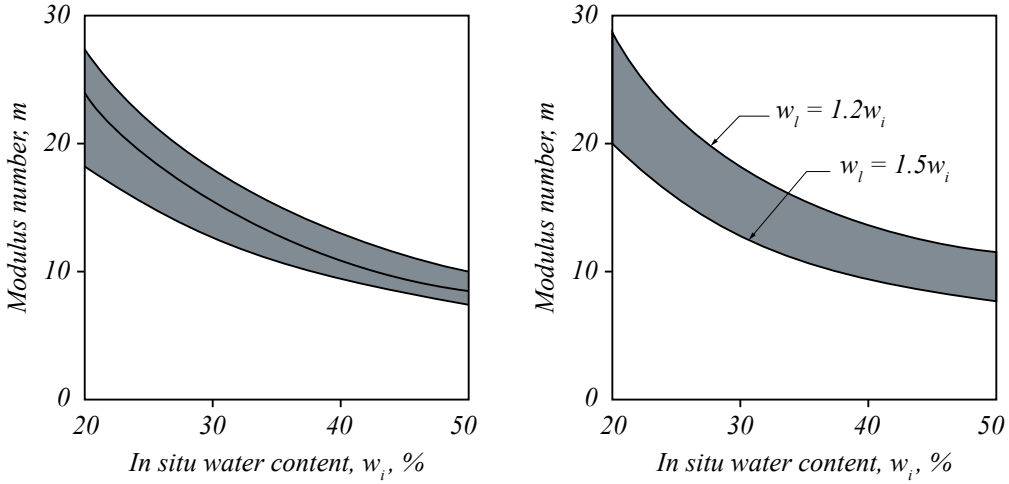


Figure 6-6 Relationship between modulus number for primary (virgin) loading and natural water content for Norwegian sensitive clays (Karlsrud and Hernandez-Martinez 2013).

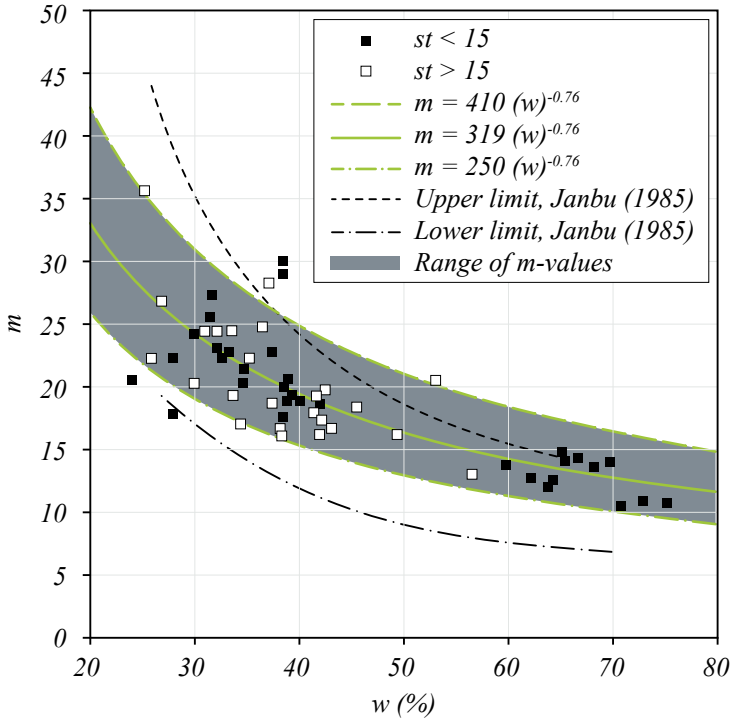

## 6.3. Non-linear constrained modulus formulation for sand and silt

The constrained modulus is non-linear and also depends on the stress history, i.e., virgin loading versus unloading and reloading. The constrained tangential modulus can be expressed by the following non-linear formulation (Andersen & Schjetne 2013):

$$M_l = m_l p^{ref} \left( \frac{\sigma_v'}{p^{ref}} \right)^{n_l} \quad (17)$$

$$M_u = m_l p^{ref} \left( \frac{\sigma_{v,max}'}{p^{ref}} \right)^{n_l} m_u \left( \frac{\sigma_v'}{\sigma_{v,max}'} \right)^{n_u} \quad (18)$$

$$M_r = m_l p^{ref} \left( \frac{\sigma_{v,max}'}{p^{ref}} \right)^{n_l} m_r \left( \frac{\sigma_v'}{\sigma_{v,max}'} \right)^{n_r} \quad (19)$$

where:

1. $M_l, M_u, M_r$ are the tangential constrained modulus for first loading (virgin), unloading, and reloading, respectively
2. $m_l, m_u, m_r$ are the constrained modulus numbers for first loading (virgin), unloading, and reloading, respectively
3. $n_l, n_u, n_r$ are the exponents for first loading (virgin), unloading, and reloading, respectively
4. $p^{ref} = p_a$ = atmospheric pressure (≈100 kPa)
5. $\sigma_v'$ is the vertical effective stress
6. $\sigma_{v,max}'$ is the maximum vertical effective stress prior to unloading

The formulation for virgin loading was proposed for sand by Janbu (1963), who used an exponent of $n$ = 0.5. A modification to this exponent is proposed by Andersen (2015).

Andersen & Schjetne (2013) presented parameter correlations for sands and silts for the proposed formula. The modulus number for virgin loading can be defined as a function of water content and fines content, as shown in Figure 6-7.

Figure 6-7 Modulus number for virgin loading for sand and silt as a function of fines content and water content (Andersen 2015).

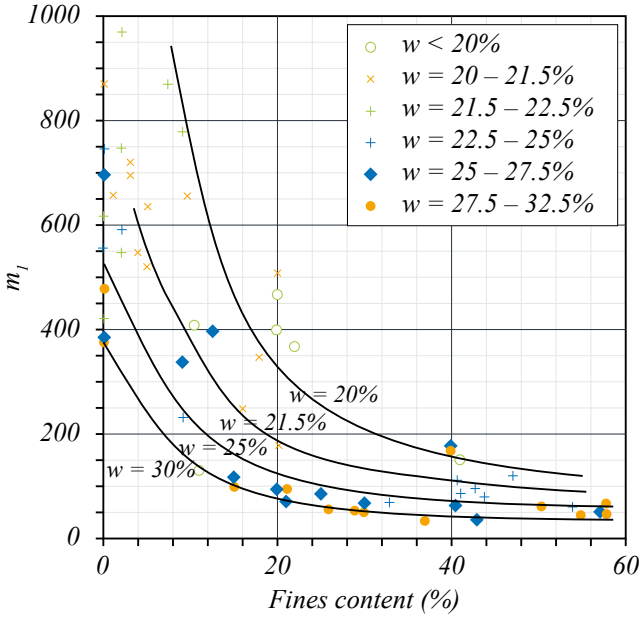

Andersen (2015) suggested correlations for unloading and reloading modulus numbers $m_u$ and $m_r$ as a function of ml as illustrated in Figure 6-8. The correlations are valid for exponent values of $n_l$ = 0.65, $n_u$ = 1.05 and $n_r$ = 0.1. The average ratio between modulus numbers for unloading and reloading is 2.87, with a standard deviation of 0.78.

Figure 6-8 Modulus number for unloading (left) and reloading (right) as functions of modulus number for virgin loading (Andersen 2015).

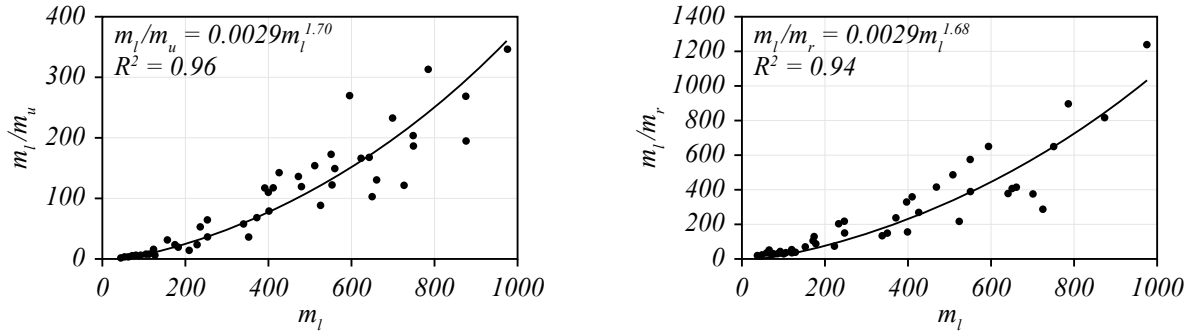

# 7. SOIL MODULUS FROM IN-SITU TESTING

## 7.1. Applicability of in-situu testing

Table 7-1 presents a summary of the current perceived applicability of the major in-situ tests: the Cone Penetration Test (*CPT*), and its recent variations (e.g., CPTu and SCPTu), have the widest application for estimating geotechnical parameters over a wide range of materials from very soft soil to weak rock. In contrast, the Standard Penetration Test (*SPT*) has less applicability and accuracy in evaluating soil parameters.

It is worth noticing that seismic tests (e.g., SCPTu, SDMT) are considered the most reliable in-situ testing to derive the soil stiffness parameters as they link the stiffness parameters to the measured shear wave velocity. This aspect is discussed in section 2.

Table 7-1 Perceived applicability of in-situ testing (Mitchell et al., 1978 and Lunne et al. 1997).

| Group | In-situ Test | Geotechnical Parameter | | | | | | | | | | | | Ground Type | | | | | |
|---|---|---|---|---|---|---|---|---|---|---|---|---|---|---|---|---|---|---|---|
| | | Soil type | Profile | $u_0$ | OCR | $D_{R\text{-}\psi}$ | $\varphi'$ | $s_u$ | $G_0$-$E$ | $\sigma$-$\varepsilon$ | $M$-$C_c$ | $k$ | $c_v$ | Hard rock | Soft rock | Gravel | Sand | Silt/Clay | Peat-organic |
| Penetrometer/Direct Push | Dy. Probing (*DP*) | C | B | - | C | C | C | C | C | - | - | - | - | - | C | B | A | B | B |
| | SPT | B | B | - | C | B | C | C | C | - | - | - | - | - | C | B | A | B | B |
| | CPT | B | A | - | B | B | B | B | B | C | C | C | - | - | B | B | A | A | A |
| | CPTu | A | A | A | B | A | B | A | B | C | B | A | A | - | B | B | A | A | A |
| | SCPTu | A | A | A | A | A | B | A | A | B | B | A | A | - | B | B | A | A | A |
| | DMT | B | B | B | B | C | B | B | B | C | B | C | B | - | C | C | A | A | A |
| | SDMT | B | B | B | A | B | B | B | A | B | B | C | B | - | C | C | A | A | A |
| | Full-flow (T/ball) | C | B | B | B | C | C | A | C | C | C | C | C | - | - | - | C | B | A |
| | Field vane (FVT) | B | C | - | B | - | - | A | - | - | - | - | - | - | - | - | - | A | B |
| Pressure-meter | Pre-bored | B | B | - | C | C | C | B | B | C | C | - | C | A | A | B | B | B | B |
| | Self-bored | B | B | A | B | B | B | B | A | A | B | B | A[1] | - | C | - | B | A | B |
| | Full-displacement | B | B | B | C | C | C | B | A | A | B | B | A | - | C | - | B | A | A |
| Other | Screw/plate load | C | - | - | B | C | C | B | B | B | B | C | C | C | A | B | B | B | B |
| | Borehole shear | C | - | - | - | - | B | C | - | - | - | - | - | C | B | C | C | C | - |
| | Permeameter | C | - | A | - | - | - | - | - | - | - | A | B | A | A | A | A | A | B |
| | Borehole seismic | C | C | - | B | C | - | - | A | C | - | - | - | A | A | A | A | A | B |
| | Surface seismic | - | C | - | B | C | - | - | A | C | - | - | - | A | A | A | A | A | A |
| | Hydraulic fracture | - | - | B | - | - | - | - | - | - | - | C | C | B | B | - | - | B | C |

**Applicability:** A = High, B = Moderate, C = Low, - = None

**Geotechnical parameters:** $u_0$ = in-situ static pore pressure, OCR = over-consolidation ratio, $D_{R\text{-}\psi}$ = relative density and/or state paremeter, $\varphi'$ = peak friction angle, $s_u$ = undrained shear strength (peak and/or remolded), $G_0$-$E$ = small strain shear and/or Young's modulus, $\sigma$-$\varepsilon$ = stress-strain relationship, $M$-$C_c$ = constrained modulus and/or compression index, $k$ = permeability, $c_v$ = coefficient of consolidation.

$\varphi'$ will depend on soil type; [1] only when pore pressure sensor fitted.

## 7.2. Estimation of soil modulus from geophysical measurements

Geophysical investigations are considered one of the most reliable in-situ testings to estimate the soil stiffness parameters (Table 7-1). There are several geophysical investigation methods used in subsurface exploration which provide the shear and/or compression ($v_s$, $v_p$) waves measurement profiles. The aspects related to testing methods and procedures will not be discussed herein as this is beyond the scope of the present report.

The shear wave velocity ($v_s$) is directly related to the shear modulus and can be used to obtain $G_{max}$ and, in turn, use that to derive Emax (see Chapter 4)

The compression wave velocity is greater than the shear wave velocity, with the ratio depending on Poisson's ratio of the material. Because the strain levels associated with the propagation of seismic waves through the ground are very small for most seismic methods, the constrained and shear modulus correspond to the initial tangent (i.e., maximum) stiffness. These simple, fundamental equations are the basis of one of the most attractive features of seismic methods. In-situ compression and shear wave velocity measurements may be used to directly measure the small-strain modulus of soil and rock, which are useful for evaluating deformations related to serviceability limit states.

**In saturated soils, the measured compression wave velocity often reflects the properties of the pore fluid in the voids (Allen et al. 1980). As such, measurements of compression wave velocity in saturated soils are often of limited value for determining the properties of the soil itself. In these cases, the shear wave velocity is a more useful quantity because it is mostly unaffected by the presence of fluid in the voids.**

Table 7-2 summarizes the correlations between the soil stiffness modulus and shear wave velocity.

Table 7-2 Correlations between the soil stiffness modulus and compression and shear waves velocity.

| Parameter | In-situ test | Soil type | Interpretative Relationship | Reference |
|---|---|---|---|---|
| $G_{max}$ | Geophysical | All | $G_{max} = p_t v_s^2$ | Elastic theory |
| $E_{max}$ | Geophysical | All | $E_{max} = 2G_{max}(1+\nu) = 2\left(p_t v_s^2\right)(1+\nu)$ | Elastic theory |

## 7.3. Evaluation of soil modulus from Cone Penetration Testing (CPT)

Most piezocone penetration testing (CPTu) systems today includes cone tip resistance ($q_c$), sleeve friction ($f_s$), and pore pressure measured behind the sleeve ($u_2$). The addition of shear wave velocity ($v_s$) is also becoming increasingly popular and useful (seismic CPTu, SCPTu), particularly for evaluating the soil stiffness parameters. It is important to take into account the correction of the measured qc for unequal end area effect:

$$q_t = q_c + (1 - a_n) u_2 \quad (20)$$

Robertson (1990) proposed using normalized cone parameters, $Q_t$, $F_r$, $B_q$, to estimate soil behavior type, where:

$$Q_t = \frac{(q_t - \sigma_{v0})}{\sigma'_{v0}} \quad (21)$$

$$F_r = \frac{f_s}{(q_t - \sigma_{v0})} \quad (22)$$

$$B_q = \frac{(u_2 - u_0)}{q_t - \sigma_{v0}} \quad (22)$$

Where:
$\sigma_{v0}$ = in-situ total vertical stress;
$\sigma'_{v0}$ = in-situ effective vertical stress;
$u_0$ = in-situ equilibrium water pressure;
$\Delta_u$ = excess porewater pressure = ($u_2$-$u_0$).

Figure 7-1 Basic setup and equipment for piezocone testing.

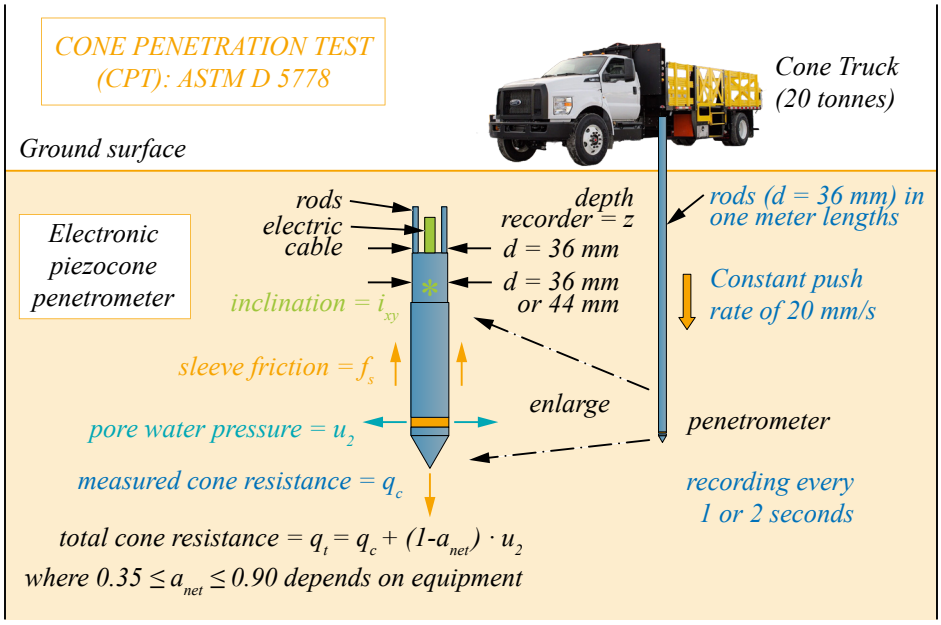


Source: Paul Mayne

Robertson et al. (1986) and Robertson (1990) introduced a Soil Behavior Type (SBT) to identify the soil behavior based on the measured CPTu (SBT) and normalized CPTu (SBTn) data. The charts are illustrated in Figure 7-2.

Figure 7-2 Soil Behavior Type (SBT and SBTn) chart (Robertson 2009).

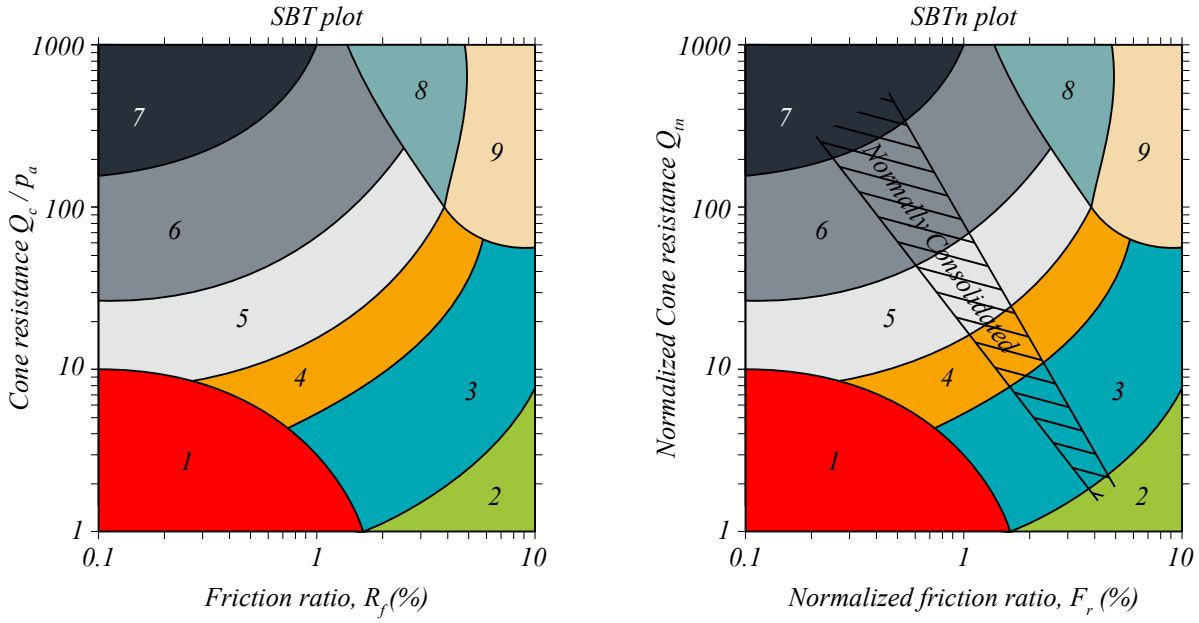


| SBT Zone | Proposed common SBT description |
|---|---|
| 1 | Sensitive fine-grained |
| 2 | Clay - organic soil |
| 3 | Clays: clay to silty clay |
| 4 | Silt mixtures: clayey silt to silty clay |
| 5 | Silt mixtures: silty sand to sandy silt |
| 6 | Sands: clean sands to silty sands |
| 7 | Dense sand to gravelly sand |
| 8 | Stiff sand to clayey sand* |
| 9 | Stiff fine-grained* |

* Oversonsolidated or cemented

Jefferies and Davies (1993) introduced a soil behavior type index $I_c$:

$$I_c = \left[ \left(3.47 - logQ_{t1}\right)^2 + \left(logF_r + 1.22\right)^2 \right]^{0.5} \quad (24)$$

This parameter is extremely useful for identifying the soil type and behavior: as an example, $I_c$ < 2.6 indicates coarse-grained soils, while $I_c$ > 2.6 identifies fine-grained soils (Figure 7-3).

Figure 7-3 Contours of $I_c$ on normalized Soil Behavior Type (SBT) chart (Robertson 2009).

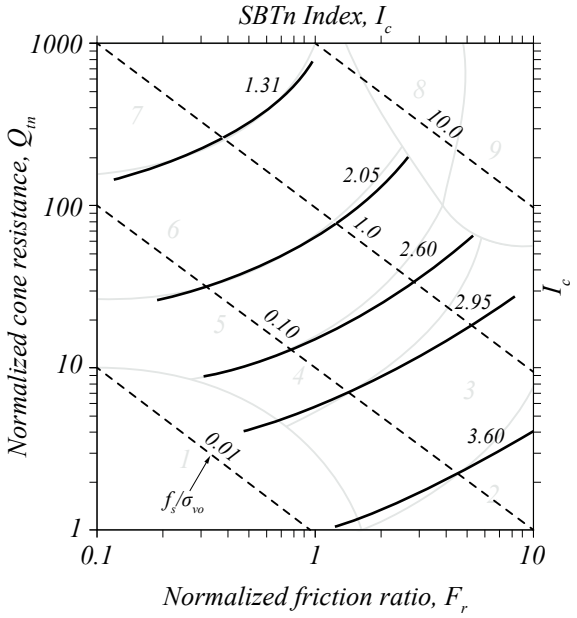


### 7.3.1 Coarse-grained soils

#### 7.3.1.1 Small strain shear modulus, $G_0$

The CPTu provides a fairly good estimation of the shear modulus in soils at low shear strain levels (< $10^{-4}$ %). Robertson (2009) proposed a chart using the shear wave velocity, $v_s$, contour on top of the SBT chart to estimate $G_0$ based on the small strain shear modulus number $K_G$ where:

$$G_0 = K_G p_a \left(\sigma'_{v0} / p_a\right)^n \quad (25)$$

Where $p_a$ is the atmospheric pressure and $n$ is a stress exponent, which can be assumed to equal 0.5 for coarse-grained soils.

Similarly, $G_0$ can be estimated based on the net cone tip resistance, such as:

$$G_0 = \alpha_G \left(q_t - \sigma_{v0}\right) \quad (26)$$

where $\alpha_G$ is the shear modulus factor.

Robertson (2009) proposed a contour chart based on the Soil Behavior Type (SBT) classification to estimate both $K_G$ and $\alpha_G$ from the CPTu data (Figure 7-4).

Figure 7-4 Contours of small strain modulus number, $K_G$ (thick solid lines), and modulus factor $\alpha_G$, on normalized SBTn $Q_{tn}$ – $F_r$ chart for uncemented Holocene- and Pleistocene-age sandy soils (After Robertson, 2009).

$$G_o = K_G \cdot P_a \cdot (\sigma'_{vo}/P_a)^{0.5}$$

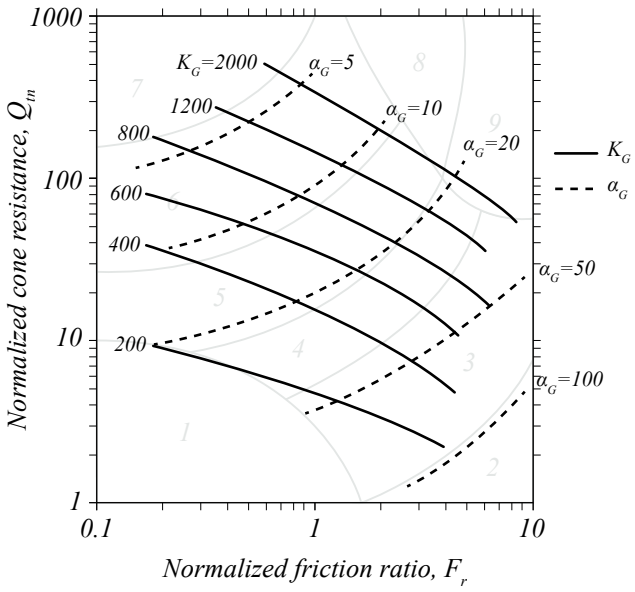


In addition, it is possible to estimate $G_0$ for young, uncemented soils using:

$$G_0 = 0.0188\left[10^{(0.55I_c+1.68)}\right](q_t - \sigma_{v0}) \quad (27)$$

Which provides a simplified means to estimate $G_0$ over a wide range of soils. These relationships are less accurate in the case of fine-grained soils as $f_s$, and hence $F_r$, is strongly influenced by soil sensitivity.

Rix and Stokoe (1991) proposed a correlation for quartz sands with the CPT point resistance $q_c$:

$$\frac{G_{max}}{p_a} = 290\left(\frac{q_c}{p_a}\right)^{0.25}\left(\frac{\sigma'_M}{p_a}\right)^{0.375} \quad (28)$$

where $\sigma'_M$ is the mean effective stress.

### 7.3.1.2 Young's modulus, *E'*

The drained Young's modulus $E'$ is linked to the shear modulus as:

$$E' = 2(1+\nu)G \quad (29)$$

Where $\nu$ is the Poisson's ratio, which ranges between 0.1 and 0.35 for most of the soils in drained conditions, thus giving:

$$E' \sim 2.5G \quad (30)$$

In addition, it is possible to estimate $E'$ from $G_0$. For this purpose, there is a need to adjust the $G_0$ to a strain level appropriate to the design purposes. Fahey and Carter (1993) and Mayne (2005) suggested a simplified approach to estimate Young's modulus for many design applications in simplified elastic solutions:

$$E' \sim 0.8G_0 \quad (31)$$

**Using this ratio, corresponding to ≈0.1% strain**, Robertson (2009) and Robertson and Cabal (2015) proposed two correlations to estimate $E'$ based on CPT data, such as:

$$E' = K_E p_a \left(\sigma'_{v0} / p_a\right)^n \quad (32)$$

$$E' = \alpha_E \left(q_t - \sigma_{v0}\right) \quad (33)$$

Where $K_E$ is Young's modulus number while $\alpha_E$ is Young's modulus factor $\alpha_E$, both factors can be derived from the SBT contours chart illustrated in Figure 7-5.

Figure 7-5 Contours of Young's modulus number, $K_E$ (thick solid lines) and modulus factor $\alpha_E$, on normalized SBTn $Q_{tn} - F_r$ chart for uncemented Holocene- and Pleistocene-age sandy soils (after Robertson, 2009).

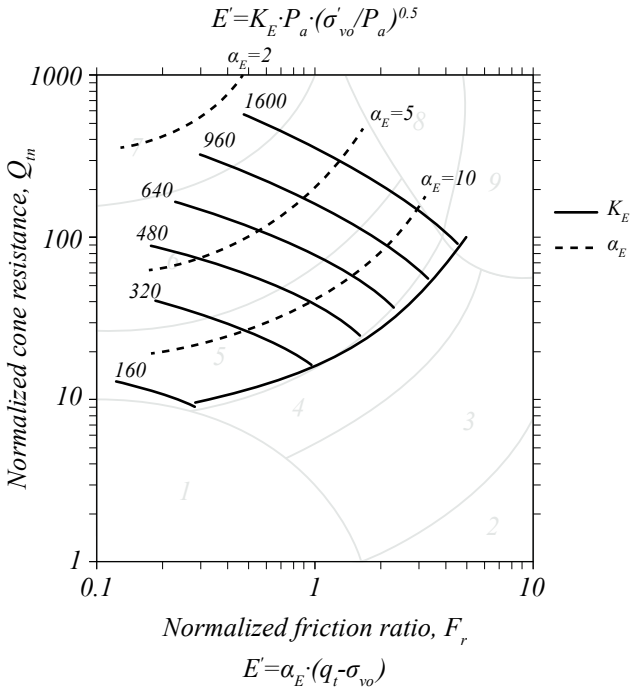


In addition, Robertson (2009) proposed a CPTu based correlation to estimate $E'$ for uncemented, predominately silica-based soils of either Holocene or Pleistocene age ($I_c$ < 2.6):

$$E' = 0.015\left[10^{(0.55 I_c + 1.68)}\right]\left(q_t - \sigma_{v0}\right) \quad (34)$$

Robertson and Campanella (1983) proposed a relationship between the cone tip resistance $q_c$ from CPT and the drained secant modulus $E_{50}$ and $E_{25}$ for sands (Figure 7-6).

Figure 7-6 Cone resistance $q_c$ versus secant $E_{25}$ and $E_{50}$ modulus for sands (after Robertson and Campanella 1983).

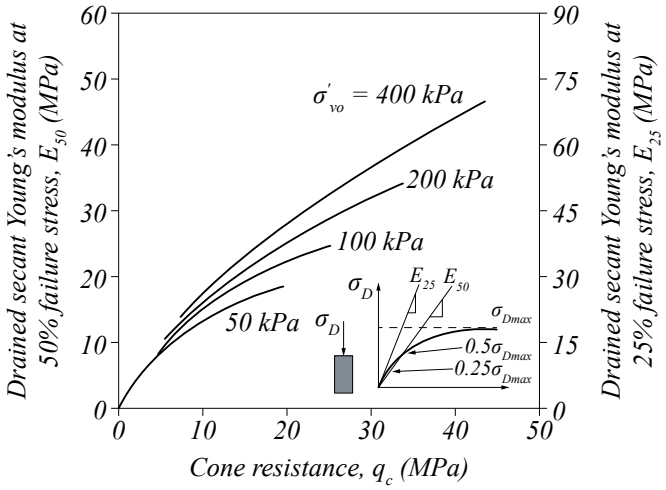


Several additional correlations have been proposed in the literature. They are summarized in Table 3.1.

#### 7.3.1.3 Constrained modulus, $M$

Existing correlations between constrained modulus $M$ and cone resistance typically have the form:

$$M = \alpha_M \left( q_t - \sigma_{v0} \right) \quad (35)$$

The factor $\alpha_M$ varies with soil type, plasticity, and natural water content. Mayne (2007) proposed $\alpha_M$ values ranging between 1 and 10, where the low values apply to soft clays.

Robertson (2009) suggested the following simplified correlation for coarse-grained soil ($I_c$ < 2.2):

$$\alpha_M = 0.03\left[ 10^{(0.55 I_c + 1.68)} \right] \quad (36)$$

Table 7-3 summarizes the most common correlations to evaluate the soil stiffness modulus in coarse-grained soils based on CPTu data.

Table 7-3 Summary of soil modulus correlations from CPTu for coarse-grained soils.

| Parameter | In-situ test | Soil type | Interpretative Relationship | Reference |
|---|---|---|---|---|
| $G_0$ | CPT | Coarse-grained soils | $G_0 = K_E p_a \left(\sigma'_{v0} / p_a\right)^n$<br>Where:<br>$K_G$: small strain shear modulus number determined from CPTu data (Robertson 2009)<br>$p_a$: atmospheric pressure<br>$n$: stress exponent (= 0.5 for coarse-grained soils) | Robertson (2009) |
| $G_0$ | CPT | Coarse-grained soils | $G_0 = \alpha_G \left(q_t - \sigma_{v0}\right)$<br>Where:<br>$\alpha_G$: shear modulus factor determined from CPTu data (Robertson 2009)<br>$q_t$: corrected cone tip resistance | Robertson (2009) |
| $G_0$ | CPT | Coarse-grained soils ($I_c$ < 2.60) | $G_0 = 0.0188\left[10^{(0.55I_c+1.68)}\right]\left(q_t - \sigma_{v0}\right)$<br>Where:<br>$I_c$: soil behavior type index<br>$q_t$: corrected cone tip resistance | Robertson (2009) |
| $E'$ | CPT | Coarse-grained soils | $E' = K_E p_a \left(\sigma'_{v0} / p_a\right)^n$<br>Where:<br>$K_E$: Young's modulus number was determined from CPTu data (Robertson 2009)<br>$p_a$: atmospheric pressure<br>$n$: stress exponent (= 0.5 for coarse-grained soils) | Robertson (2009) |
| $E'$ | CPT | Coarse-grained soils | $E' = \alpha_E \left(q_t - \sigma_{v0}\right)$<br>Where:<br>$\alpha_E$: Young's modulus factor determined from CPTu data (Robertson 2009)<br>$q_t$: corrected cone tip resistance | Robertson (2009) |
| $E'$ | CPT | Coarse-grained soils ($I_c$ < 2.60) | $E' = 0.015\left[10^{(0.55I_c+1.68)}\right]\left(q_t - \sigma_{v0}\right)$<br>Where:<br>$I_c$: soil behavior type index<br>$q_t$: corrected cone tip resistance | Robertson (2009) |
| $E'$ | CPT | Clays, silts, sands | $E' = 5\left(q_t - \sigma_{v0}\right)$ | Mayne (2007) |
| $E'$ | CPT | Sandy soils (normally consolidated) < 100 years | $E' = \left(2.5 \text{ to } 5\right) q_c$ | Briaud (2013) |
| $E'$ | CPT | Sandy soils (normally consolidated) > 3000 years | $E' = \left(3.5 \text{ to } 6\right) q_c$ | Briaud (2013) |
| $E'$ | CPT | Sand: $q_c$ < 5 MPa | $E' = 2q_c$ | Briaud (2013) |
| $E'$ | CPT | Sand: $q_c$ > 10 MPa | $E' = 1.5q_c$ | Briaud (2013) |
| $M_0$ | CPT | Coarse-grained soils | $M = \alpha_M \left(q_t - \sigma_{v0}\right)$<br>Where:<br>5 < $\alpha_M$ < 10 | Mayne (2007) |
| $M_0$ | CPT | Coarse-grained soils ($I_c$ < 2.2) | $M = \alpha_M \left(q_t - \sigma_{v0}\right)$<br>Where:<br>$\alpha_M = 0.03\left[10^{(0.55I_c+1.68)}\right]$ | Robertson (2009) |

Note:

a) $p_a$ = atmospheric pressure (= 1 bar = 100 kPa)

### 7.3.2 Fine-grained soils

#### 7.3.2.1 Constrained modulus, $M$

Robertson (2009) proposed a contour of the constrained modulus number, $K_M$, on the normalized SBT chart, giving the possibility to estimate $M$ as:

$$M = K_M p_a \left(\sigma'_{v0} / p_a\right)^a \quad (37)$$

Where $a$ is the stress exponent, which is equal to 1 for stresses above the pre-consolidation stress and equal to 0 for stresses below the pre-consolidation stress, thus obtaining:

$$M = K_M p_a \quad (38)$$

Figure 7-7 Contours of constrained modulus number, $K_M$ on normalized SBTn $Q_{tn} - F_r$ chart (after Robertson, 2009).

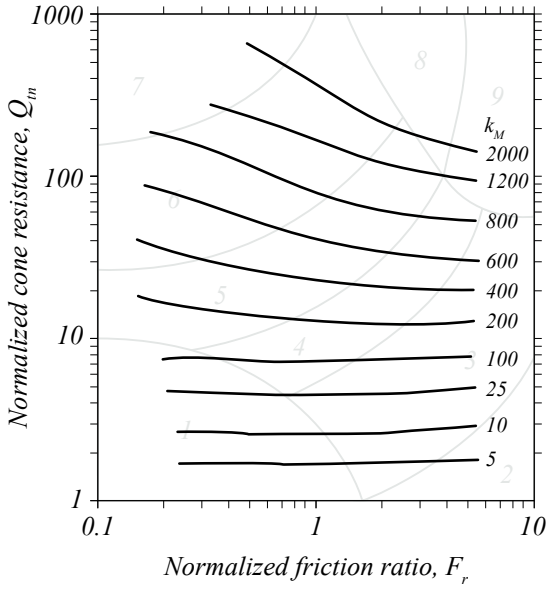


For fine-grained soils, $K_M$ varies between 5 and 100 (zone 1,2, 3).

As previously observed, existing correlations between $M$ and the cone resistance typically have the form:

$$M = \alpha_M \left(q_t - \sigma_{v0}\right) \quad (39)$$

Exploiting the data from fine-grained soils, Mayne (2007) indicated values of $\alpha_M$ varying between 1 and 10, where the lowest values apply to soft clays. Di Buò et al. (2018) suggested values varying from 5 to 10 for Finnish clays.

Robertson (2009) proposed the following $\alpha_M$ values for fine-grained soils:
$\alpha_M = Q_{tn}$ when $Q_{tn} \leq 14$
$\alpha_M = 14$ when $Q_{tn} > 14$

which provides fairly good estimation when compared with laboratory data from different soft clays sites.

Table 7-4 Summary of constrained modulus correlations from CPTu for fine-grained soils.

| Parameter | In-situ test | Soil type | Interpretative Relationship | Reference |
|---|---|---|---|---|
| $M$ | CPT | Fine-grained soils $\sigma_v > \sigma_p$ | $M = K_M p_a \left(\sigma'_{v0} / p_a\right)^a$<br>Where:<br>$K_M$: constrained modulus number<br>$a$ = 1 for $\sigma v > \sigma p$ | Robertson (2009) |
| $M$ | CPT | Fine-grained soils $\sigma_v < \sigma_p$ | $M = K_M p_a$ | Robertson (2009) |
| $M$ | CPT | Fine-grained soils | $M = \alpha_M \left(q_t - \sigma_{v0}\right)$<br>Where:<br>$1 < \alpha_M < 5$ | Mayne (2007) |
| $M$ | CPT | High sensitive clays | $M = \alpha_M \left(q_t - \sigma_{v0}\right)$<br>Where:<br>$5 < \alpha_M < 10$ | Di Buò (2020) |
| $M$ | CPT | Fine-grained soils ($I_c > 2.2$) | $M = \alpha_M \left(q_t - \sigma_{v0}\right)$<br>Where:<br>$\alpha_M = Q_{tn}$ when $Q_{tn} \leq 14$<br>$\alpha_M = 14$ when $Q_{tn} > 14$ | Robertson (2009) |

#### 7.3.2.2 Small strain shear modulus, $G_0$

For clay, Mayne and Rix (1993) proposed:

$$\frac{G_{max}}{p_a} = 100\left(\frac{q_c}{p_a}\right)^{0.695} e^{-1.13} \qquad (40)$$

where $e$ is the void ratio.

## 7.4. Evaluation of soil modulus from Standard Penetration Testing (SPT)

One of the oldest and most widely used in situ tests is the SPT. The SPT test is generally used to estimate the shear strength parameters of sandy soils and overconsolidated clays. It is unreliable for soils containing course gravel, cobbles, boulders, cohesionless silts, and soft and sensitive clays. Figure 7-8 depicts the general layout of the SPT using a hammer system, drill rods, and split-spoon or split-barrel sampler.

The basic testing procedure consists of driving a hollow steel tube with an outside diameter of 2.0 in. (51 mm) and an inside diameter of 1.38 in. (35 mm) into the ground at a vertical distance of 18 in. (46 cm) and counting the number of blows required to drive each 6-in. (15-cm) increment. The first increment is considered a seating of the sampler. The blows obtained for the second and third increments are summed to give an $N$-value, which is reported in blows per foot (bpf). The test is typically conducted at 5-ft (1.5-m) depth intervals. At shallow depths of less than 10 ft (3 m), the depth intervals are often less (e.g., 2.5-ft [0.75-m] intervals).

Figure 7-8 SPT setup and procedure.

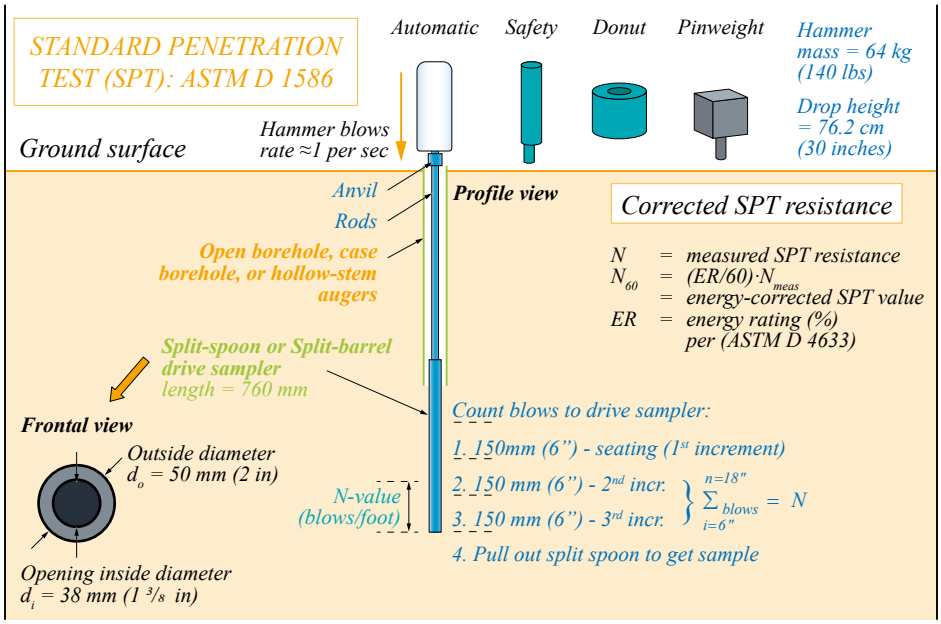


### 7.4.1 Correction factors

Most of the SPT based correlations available in the literature are based on the $N_{60}$ reference value, which takes into account the average energy efficiency of SPT, and it is defined as follows:

$$N_{60} = C_E N_m = \left(\frac{ER}{60}\right) N_m \qquad (41)$$

where:
$C_E$ = correction factor for hammer energy
$N_m$ = measured blow count

In addition to hammer energy ($C_E$), the N-value is also affected by factors such as borehole diameter ($C_B$), rod length and type ($C_R$), and sampler configuration ($C_S$). Therefore, the corrected $N_{60}$ is calculated by adjusting the measured blow counts using the following relation:

$$N_{60} = C_E C_B C_R C_S N_m \qquad (42)$$

Approximate values for the various correction factors are given in Table 7-5.

Table 7-5 SPT correction factors for field procedures.

| Parameter | Influencing variable | Field case | Factor values |
|---|---|---|---|
| $C_N$ | Depth effect due to increasing effective overburden stress ($\sigma'_{v0}$) | $\sigma_{atm}$ = 1 atmosphere = 1.013 bars = 101.3 kilopascals = 1.058 tsf = 14.7 psi | $C_N = (\sigma_{atm} / \sigma'_{v0}) 0.5 \leq 2$ |
| $C_E$ | $C_E = ER/60$ where $ER$ = hammer energy ratio (ASTM D4633) | Hammer Type | $C_E$ = 1.0 to 1.6; (Hammer type: automatic)<br>$C_E$ = 0.8 to 1.3; (Hammer type: safety)<br>$C_E$ = 0.6 to 0.8; (Hammer type: donut)<br>$C_E$ = 0.5 to 0.7; (Hammer type: pinweight) |
| $C_B$ | Borehole diameter ($b$, inches) | Borehole diameter | $C_B$ = 1.0; ($2.5 \leq b \leq 4.5$)<br>$C_B$ = 1.05 ($b$ = 6)<br>$C_B$ = 1.15 ($b$ = 8) |
| $C_S$ | Split-barrel sampler | Split-barrel sampler | $C_S$ = 1.0; (with liner)<br>$C_S$ = 1.2 (no liner) |
| $C_R$ | Drill rod length, $L$ (ft) | Drill rod length | $C_R$ = 1.0; ($L > 33$)<br>$C_R$ = 0.95 ($20 < L < 33$)<br>$C_R$ = 0.85 ($13 < L < 20$)<br>$C_R$ = 0.80 ($10 < L < 13$)<br>$C_R$ = 0.75 ($L < 10$) |

*Source: modified from Skempton (1986), Kulhawy and Mayne (1990), Youd et al. (2001).*

### 7.4.2 Shear wave velocity evaluation based on SPT

In the case of conventional SPTs, the in-situ shear wave velocity vs can be estimated by using the $N_{60}$ factor, as shown in Figure 7-9:

$$v_s\,(m/s) = 97\,(N_{60})^{0.314} \qquad (43)$$

Figure 7-9 Estimation of vs based on SPT.

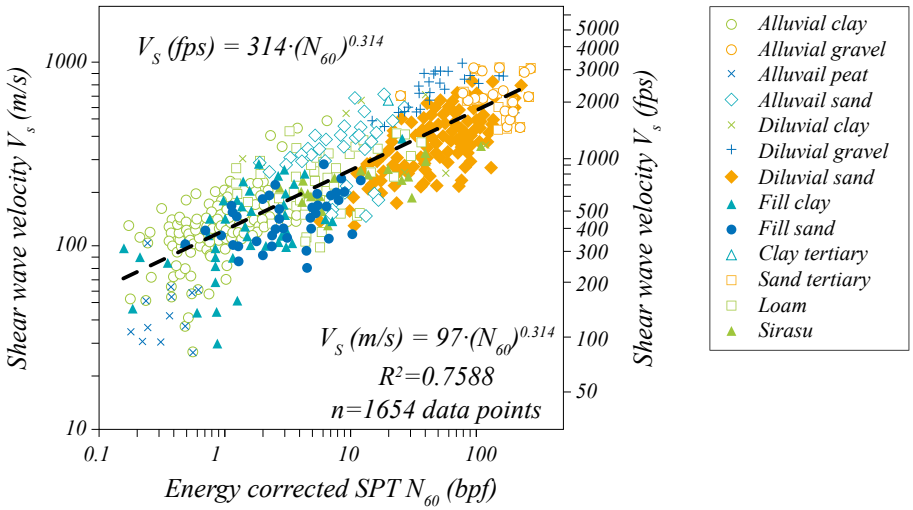


*Source: data from Imai and Tonouchi (1982)*

The possibility of estimating $\nu_s$ is useful to evaluate the soil modulus as discussed in section 2.

### 7.4.3 Evaluation of soil modulus based on SPT

A number of correlations are proposed in the literature to evaluate the soil modulus from SPT data. A summary of the existing correlations from the literature is presented in Table 7-6.

Table 7-6 Summary of SPT correlations for Young's modulus in coarse-grained soils.

| Parameter | In-situ test | Soil type | Interpretative Relationship | Reference |
|---|---|---|---|---|
| $E'$ | SPT | Silts, sandy silts, slightly cohesive mixtures | $E\ (kPa)=400\ N$ | Briaud (2013) |
| $E'$ | SPT | Silts, sandy silts, slightly cohesive mixtures | $E\ (kPa)=400\ N$ | Briaud (2013) |
| $E'$ | SPT | Clean fine to medium sands and slightly silty sands | $E\ (kPa)=700\ N$ | Briaud (2013) |
| $E'$ | SPT | Coarse sand and sand with little gravel | $E\ (kPa)=1000\ N$ | Briaud (2013) |
| $E'$ | SPT | Sandy gravels and gravels | $E\ (kPa)=1200\ N$ | Briaud (2013) |
| $E'$ | SPT | Sand (normally consolidated) | $E\ (kPa)=7000\ [N]^{0.5}$<br>$E\ (kPa)=(1500\ to\ 22000)\ \log_e [N]$<br>$E\ (kPa)=500\ (N+15)$ | Briaud (2013) |
| $E'$ | SPT | Sand (saturated) | $E\ (kPa)=250\ (N+15)$ | Briaud (2013) |
| $E'$ | SPT | Sand (overconsolidated) | $E\ (kPa)=4000+1050\ N$ | Briaud (2013) |
| $E'$ | SPT | Gravelly sand | $E\ (kPa)=1200\ (N+6)$ | Briaud (2013) |

** SPT blow count $N$ in bpf (blows per foot), blows per 0.3 m.*

Ohta and Goto (1976) and Seed et al. (1986) proposed, for sands:

$$\frac{G_{max}}{p_a} = 447 N^{0.33} \left( \frac{\sigma'_M}{p_a} \right)^{0.5} \qquad (44)$$

where $N$ is the SPT blow count corrected for 60% of maximum energy and corrected to 100 kPa of pressure.

# 8. SOIL MODULUS DETERMINATION FOR FINNISH SOIL CONDITIONS

As discussed in the previous chapters, a stress-strain relationship of soils is non-linear and, hence, soil modulus is not constant, but it depends on several factors (see Chapter 3). Soil modulus, including e.g., Young's modulus $E$, shear modulus $G$ and constrained modulus $M$ can be determined from both laboratory and in-situ testing. Laboratory testing (e.g. triaxial testing) provides a full description of the stress-strain behavior, and stress or strain increments can be designed to obtain the parameters for the stress/strain range of interest. However, these are not always available, especially in small-sized projects. Furthermore, soil specimens may suffer from sample disturbance and may provide unreliable results. In-situ testing has the advantage of testing the soil in in-situ conditions. However, measurements require calibration from laboratory testing, meaning that the existing correlations potentially underlie all the uncertainties associated with retrieving and preparing soil specimens.

## 8.1. Coarse-grained soils

In Finland, Swedish Weight Sounding (painokairaus) and dynamic penetration test (puristinheijari) are the most common in-situ testing tools. CPTu has been gaining popularity in recent years, while SPT is quite seldom used. CPTu correlations specific to soft Finnish clays exist for constrained soil modulus $M$ (Di Buò 2020). Correlations between sand and silt will likely be available in the upcoming years (D'Ignazio 2022).

No direct correlations are available for soil modulus from weight-sounding and/or dynamic penetration testing. Nevertheless, the Finnish national Geotechnical Design guidelines based on Eurocode 7 (Annex n.6 in NCCI 7 by Liikennevirasto, 2017) provide reference tables to estimate soil parameters for a wide range of coarse soils (see Table 8-1, Table 8-2, Table 8-3). These include silts, sand, moraine, gravel and crushed rocks. Materials as subdivided according to their classification as loose (or very loose), medium dense or dense.

Table 8-1 Table 1 in Annex 6 in NCCI 7 (Liikennevirasto, 2017) – English translation.

| Soil type | | Unit weight $\gamma$ (kN/m$^3$) | | Friction angle $\varphi'$ (°) | Janbu's tangent modulus parameters | | Sounding resistance | | |
|---|---|---|---|---|---|---|---|---|---|
| | | Dry | Saturated | | Modulus number $m$ | Stress exponent $\beta$ | Cone resistance from dynamic penetration test (puristinheijari) $q_c$ (MPa) | Weight sounding $P_k$/0.2 m ($P_k$ = half rotations) | Blow count from dynamic penetration test (puristinheijari) $L$/0.2 m ($L$ = blows) |
| Coarse silt | Loose | 14...16 | 19... | 28 | 30...100 | 0.3 | < 7 | < 40 | < 8 |
| | Medium–dense | | | 30 | 70...150 | 0.3 | 7...15 | 40...100 | 8...25 |
| | Dense | 16...18 | 21 | 32 | 100...300 | 0.3 | >15 | >100 | > 25 |
| Fine sand $d10 < 0.06$ | Loose | 15...17 | 19... | 30 | 50...150 | 0.5 | <10 | 20...50 | 5...15 |
| | Medium–dense | | | 33 | 100...200 | 0.5 | 10...20 | 50...100 | 15...30 |
| | Dense | 16...18 | 21 | 36 | 150...300 | 0.5 | > 20 | > 100 | > 30 |
| Sand $d10 > 0.06$ | Loose | 16...18 | 20... | 32 | 150...300 | 0.5 | <6 | 10...30 | 5...12 |
| | Medium–dense | | | 35 | 200...400 | 0.5 | 6...14 | 30...60 | 12...25 |
| | Dense | 18...20 | 22 | 38 | 300...600 | 0.5 | > 14 | > 60 | > 25 |

Table 8-2 Table 2 in Annex 6 in NCCI 7 (Liikennevirasto, 2017) – English translation.

| Soil type | | Unit weight $\gamma$ (kN/m$^3$) | | Friction angle $\varphi'$ (°) | Janbu's tangent modulus parameters | | Sounding resistance | | |
|---|---|---|---|---|---|---|---|---|---|
| | | Dry | Saturated | | Modulus number $m$ | Stress exponent $\beta$ | Cone resistance from dynamic penetration test (puristinheijari) $q_c$ (MPa) | Weight sounding $P_k$/0.2 m ($P_k$ = half rotations) | Blow count from dynamic penetration test (puristinheijari) $L$/0.2 m ($L$ = blows) |
| Gravel | Loose | 17...19 | 20... | 34 | 300...600 | 0.5 | < 5.5 | 10...25 | 5...10 |
| | Medium-dense | | | 37 | 400...800 | 0.5 | 5.5...12 | 25...50 | 10...20 |
| | Dense | 18...20 | 22 | 40 | 600...1200 | 0.5 | > 12 | > 50 | > 20 |
| Moraine | Very loose | 16...19 | 20...22 | ...34 | (≤100)* 300...600 | 0.5 | < 10 | < 40 | < 20 |
| | Loose | 17...20 | 20...22 | ...36 | (100...250)* 600... | 0.5 | This | 40...100 | 20...60 |
| | Medium-dense | 18...21 | 21...23 | ...38 | 800... | 0.5 | - | > 100 | 60...140 |
| | Dense | 19...23 | 21...24 | ...40 | 1200... | 0.5 | - | Refusal | > 140 |

Note to Table 8-2: Values with asterisk* are for cases where the moraine has not been subjected to glacial overburden, i.e "normally consolidated moraine".

Table 8-3 Table 3 in Annex 6 in NCCI 7 (Liikennevirasto, 2017) – English translation.

| Grain size | Unit weight $\gamma$ (kN/m$^3$) | Modulus number $m$ | Stress exponent $\beta$ | Friction angle $\varphi'$ (°) |
|---|---|---|---|---|
| Crushed rock 0..150/0...300 | 17...22 | 500...2000 | 0.5 | 38...42 |
| Blasted rock 0...300/0...600 | 17...22 | 300...1500 | 0.5 | 38...42 |

The tables contain information on unit weight, friction angle, modulus number, and stress exponent for each soil category. The parameters are meant to be used to model drained conditions.

The data in Table 8-1 to Table 8-3 is based on studies done in Finland from the 1960's onwards (e.g. Helenelund 1964, 1966; Tammirinne 1969, Valkeisenmäki 1973). They have been part of established engineering practice in Finland from at least the 1990's onwards, when they were incorporated in official bridge design manuals and later to higher-level guidelines.

They are often referred to even in projects that are not governed by NCCI7 (i.e. projects not related to traffic infrastructure). As such, their use in Finland can be considered safe in terms of established practice. They do not have the same status outside of Finland but may still be carefully used as background reference material. Additional, locally established references may be required.

The suggested ranges for the different parameters are linked with the test results from Weight Sounding (in Finnish painokairaus) and dynamic testing (in Finnish puristinheijari). Therefore, these tables provide guidance when determining soil parameters when in-situ data or/and grain size information is available. It must be noted that some of the data in the tables overlap. It is therefore recommended to carry out at least grain size distribution analyses along with in-situ testing.

Furthermore, the rod diameter of the weight sounding may influence the measurements. As shown in Figure 8-1, the sounding resistance may be overestimated when a rod diameter of 25 mm is used (as is typical with modern geotechnical crawler rigs). The standard 22 mm diameter results appear to be in line with CPTU measurements for the site considered in Figure 8-1. As the tables in NCCI 7 were produced in the 1960's... 1990's, sounding results refer to the 22 mm diameter. This must be considered when using sounding results to estimate soil parameters from NCCI 7.

Figure 8-1 Comparison of weight sounding (painokairaus) results from 22 mm vs. 25 mm rod diameter (courtesy of FTIA / Panu Tolla, 2021).

***Painokairaus EN ISO 22476-10 (2017)***

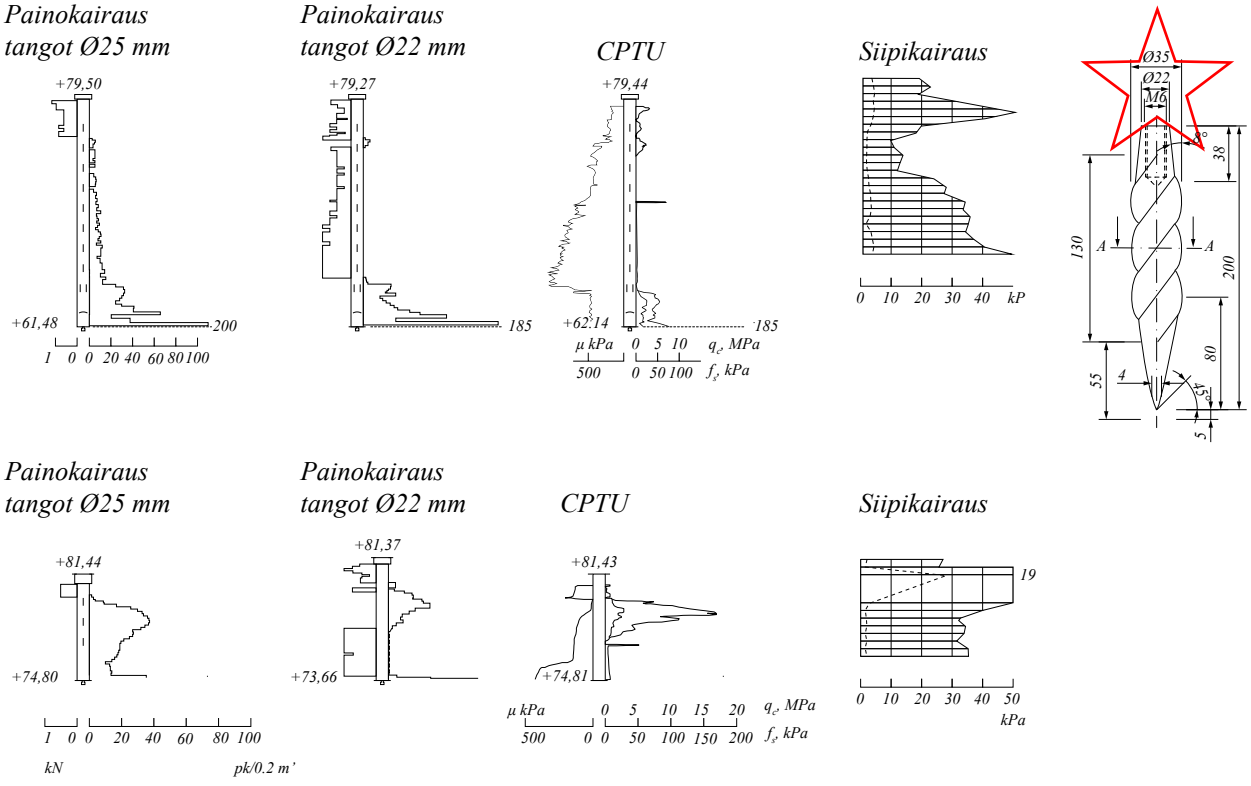


*Kairausopas I*
*Tangot*
*Tankojen mitat ovat seuraavat:*
*Ø22 mm umpitanko paino - 3,0 kg. pituus 1,0 m*
*Ø22 mm putkitanko paino - 2,0 kg. --"-- käytetään lähinnä*
*Ø25 mm umpitanko paino - 4,0 kg. --"-- vain monitoimi-*
*Ø25 mm putkitanko paino - 2,5 kg. --"-- kairayksiköissä*

In the tables, the symbol $m$ is used to indicate the modulus number from the constrained tangent modulus formulation (Janbu 1998):

$$M = mp^{ref}\left(\frac{\sigma'}{p^{ref}}\right)^{1-\beta}$$

where:

$M$ = tangent constrained modulus (kPa, MPa)
$p^{ref}$ = reference stress = 100 kPa ≈ 1 atm
$\sigma'$ = intergranular pressure, i.e. effective vertical stress (kPa, MPa)
$m$ = modulus number (dimensionless)
$\beta$ = stress exponent (dimensionless)

The constrained modulus $M$ can be referred to as $E_{oed}$. Furthermore, $m \cdot p^{ref} = E_{oed}^{ref}$. This leads to:

$$E_{oed} = E_{oed}^{ref} \left( \frac{\sigma_v'}{p^{ref}} \right)^{1-\beta}$$

Note that here, $E_{oed}$ is given as a function of vertical effective stress $\sigma_v'$. Depending on the software used, it may also be given as a function of effective mean stress $p'$. According to the tables, (1 - $\beta$) ≈ 0.5 for coarse soils, while ≈ 0.7 for silty soils.

For the onshore wind turbine gravity foundation, the secant modulus for primary loading $E_{50}$ is a parameter of interest. As discussed in section 3.2.1, $E_{50}$ depends on the confinement stress (i.e., cell pressure $\sigma_3'$) in the triaxial cell, increasing with increasing $\sigma_3'$.

Hence, $\sigma_3'$ can be used as the reference stress to define the drained secant modulus $E_{50}$. On the contrary, the constrained modulus $E_{oed}$ increases with increasing vertical stress $\sigma_v'$ or $\sigma_1'$ The stresses $\sigma_3'$ and $\sigma_1'$ can be linked by means of the lateral earth pressure coefficient at rest $K_0$ as $\sigma_3' = K_{01}'$.

Figure 8-2 shows the stress dependency of $E_{oed}$ and $E_{50}$. Given that the reference stresses are different and linked by the $K_{0nc}$, it is observed that $E_{oed} \approx E_{50}$ for $NC$ soil. This was confirmed experimentally by Schanz (1998) for sands (Figure 8-3).

Figure 8-2 Stress-dependent modulus based on the Hardening Soil model's formulation (adapted from Mansikkamäki 2015).

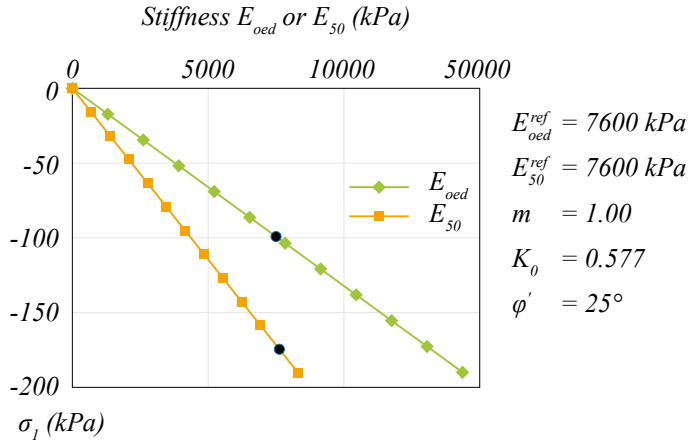


Figure 8-3 Relationship between $E_{50}^{ref}$ and $E_{oed}^{ref}$ for sands (Schanz 1998).

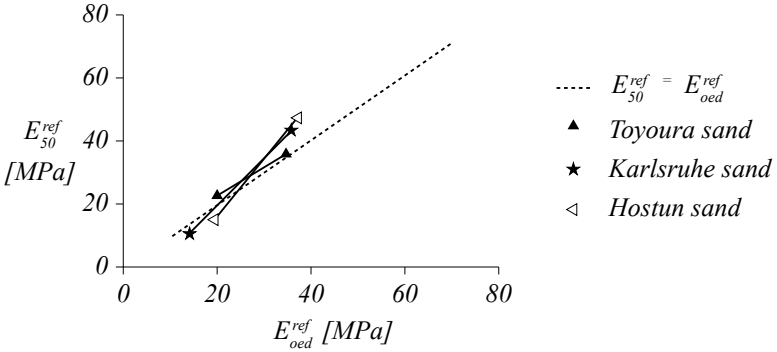


Hence, the stress-dependent secant modulus for primary loading $E_{50}$ can be defined as follows:

$$E_{50} = E_{50}^{ref} \left( \frac{\sigma_3'}{p^{ref}} \right)^{1-\beta} = m p^{ref} \left( \frac{\sigma_3'}{p^{ref}} \right)^{1-\beta}$$

Similarly, the stress-dependent unloading/reloading modulus can be defined as follows:

$$E_{ur} = E_{ur}^{ref} \left( \frac{\sigma_3'}{p^{ref}} \right)^{1-\beta}$$

Typically, when $E_{50}$ or $E_{ur}$ cannot be directly determined from experimental curves, it may be relevant for many practical cases to assume:

$$\frac{E_{ur}}{E_{50}} = 2 \text{ to } 6$$

Higher ratios can be assumed for loose sands (3 to 6) or clays (5 to 10), whereas lower for dense sands (2 to 4) or crushed aggregates (≈ 2). As discussed in chapter 5, the $E_{ur}/E_{50}$ ratio for well-compacted aggregates can be lower than 2. This may reflect the effect of compaction or preloading, resulting in an "overconsolidated" soil state. Any subsequent loading may actually be considered a reloading event.

For sand and silt, the formulation by Andersen and Schjetne (2013) described in 6.3 can be used for a preliminary estimate of unloading and reloading constrained modulus. The average of these two modulus can be used to approximate the $E_{oed,ur}$.

Table 8-4 summarizes recommended values of $E_{oed}$ at $p^{ref}$ = 100 kPa for the coarse-grained soils defined in Table 8-1 to Table 8-3. Recommendations on the $E_{oed,ur}^{ref} / E_{oed}^{ref}$ ratio are based on Andersen & Schjetne's (2013) model illustrated in section 6.3.

Table 8-4 Range of recommended $E_{oed}^{ref}$ and $E_{oed,ur}^{ref} / E_{oed}^{ref}$ for coarse-grained material based on Liikennevirasto (2017). Note that according to experimental data by Schanz (1998), $E_{50}^{ref} \approx E_{oed}^{ref}$ (see also Fig. 8-3).

| Soil type | Density | $E_{oed}^{ref}$ (MPa)* | $E_{oed,ur}^{ref} / E_{oed}^{ref}$ ** |
|---|---|---|---|
| Coarse silt | Loose | 3–10 | 8.7–20 |
| | Medium–dense | 7–15 | 6.6–11.1 |
| | Dense | 10–30 | 4.1–8.7 |
| Fine sand $d10 < 0.06$ | Loose | 5–15 | 6.6–14 |
| | Medium–dense | 10–20 | 5.4–8.7 |
| | Dense | 15–30 | 4.1–6.6 |
| Sand $d10 > 0.06$ | Loose | 15–30 | 4.1–6.6 |
| | Medium–dense | 20–40 | 3.3–5.4 |
| | Dense | 30–60 | 2.5–4.1 |
| Gravel | Loose | 30–60 | 2.5–4.1 |
| | Medium–dense | 40–80 | 2.1–3.3 |
| | Dense | 60–120 | 1.6–2.5 |
| Moraine | Very loose | (≤ 10)*** 30…60 | 2.5–8.7 |
| | Loose | (10…25)*** 60… | 2.5–8.7 |
| | Medium–dense | 80… | 2.1 |
| | Dense | 120… | 1.6 |
| Crushed rock 0..150/0…300 | – | 50–200 | 1.1–2.8 |
| Blasted rock 0…300/0…600 | – | 30–150 | 1.3–4.1 |

* Calculated at atmospheric pressure $p^{ref}$ = 100 kPa

** $E_{oed,ur}^{ref}$ calculated as the average of unloading and reloading modulus $M_u$ and $M_r$ from section 6.3 at $p^{ref}$ = 100 kPa and assuming maximum stress of $2p^{ref}$ = 200 kPa prior to unloading.

*** For cases where the moraine has not been subjected to glacial overburden, i.e "normally consolidated moraine".

Figure 8-4 illustrates an example of constrained modulus vs. stress $\sigma_1'$ for different soil types.

Figure 8-4 Constrained modulus $M$ versus vertical effective stress $\sigma_1'$ for different soil types.

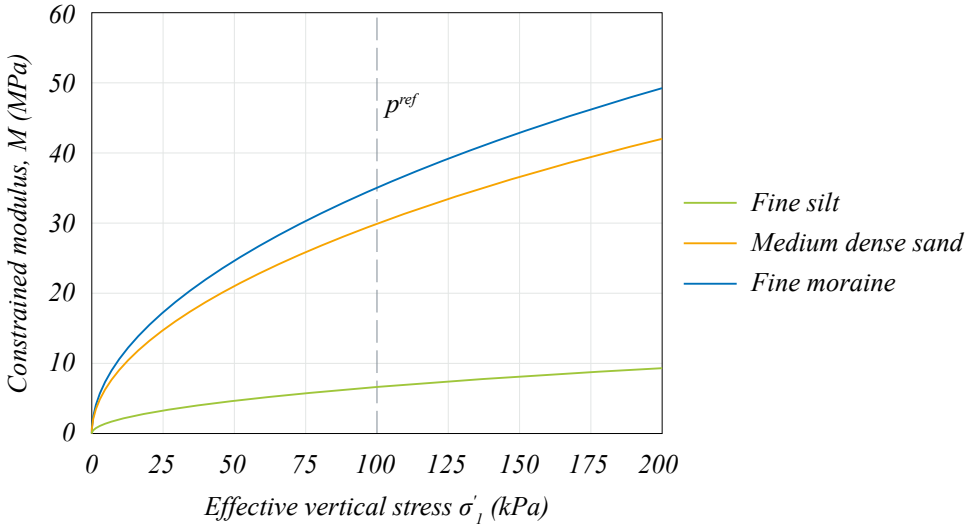


## 8.2. Fine-grained soils

Field Vane Test is the most popular in-situ tool to test undrained clays and silts in Finland. Field Vane test is used to determine the undrained shear strength $s_u$. CPTu correlations specific to soft Finnish clays exist for constrained soil modulus $M$ (Di Buò 2020). As most of the clays in Finland are soft, show apparent pre-consolidation due to aging, and especially in coastal areas can be sensitive to extra-sensitive (D'Ignazio 2016), the constrained modulus from CPTu is generally representative of the overconsolidated state. As discussed in section 6, the constrained modulus of sensitive clays is highest before reaching the pre-consolidation pressure and drops dramatically after $\sigma_c'$ and increases as a function of stress and the modulus number $m$.

Determining soil modulus in clays would require laboratory testing, e.g., triaxial or direct simple shear ($DSS$). Constrained modulus can be determined from oedometer test results. In the absence of laboratory testing, correlations based on undrained shear strength, water content, plasticity index, and over-consolidation ratio can be used for preliminary assessment. In situ tests such as weight sounding or dynamic penetration testing have not been calibrated in clays and therefore do not provide any information on parameters.

The constrained modulus of clays Eoed follows the stress-dependent modulus formulation introduced in previous sections:

$$E_{oed} = E_{oed}^{ref}\left(\frac{\sigma_v'}{p^{ref}}\right)^{1-\beta} = mp^{ref}\left(\frac{\sigma_v'}{p^{ref}}\right)^{1-\beta}$$

As discussed by Janbu (1963, 1998), the stress exponent $\beta$ for most clays tends to 0, giving $(1-\beta) \approx 1$. For extra-sensitive clays, $\beta$ can be negative, resulting in $(1-\beta) > 1$ (e.g. Länsivaara 1999). The modulus number $m$ can be estimated based on, e.g., water content, as illustrated in Figure 6-6.

The ratio $1/m$ represents the modified compression index $\lambda^*$, indicating the slope of the normally consolidated oedometer compression line in $\varepsilon$-log$\sigma$ plot. Therefore, the oedometer modulus at atmospheric pressure can be written as:

$$E_{oed}^{ref} = \frac{p^{ref}}{\lambda^*}$$

The unloading-reloading modulus is linked to the modified swelling index κ*, indicating the slope of the overconsolidated oedometer compression line in $\varepsilon$-log$\sigma'$ plot, as

$$E_{ur,oed}^{ref} = \frac{p^{ref}}{\kappa^*}$$

Literature suggests $\lambda^*/\kappa^*$ ratio varies between 5 and 10 for Finnish clays. It can be higher for extra-sensitive clays (Mansikkamäki 2015).

For a typical range of $m \approx 5–30$ in Scandinavian soft (normally consolidated) clays (Janbu 1998; Karlsrud & Hernandez-Martinez 2013; Di Buò 2020), $E_{oed}^{ref}$ = 0.5–3 MPa with $E_{oed,ur}^{ref} / E_{oed}^{ref}$ = 5–15. For overconsolidated clays with pre-consolidation pressure $\sigma_c^{'} >> \sigma_{v0}^{'} + q_F$ ($q_F$ = foundation load), the $E_{oed,ur}^{ref} / E_{oed}^{ref}$ ratio can be lower than for $NC$ clays. This is due to the higher stiffness in the $OC$ region. In that case, $E_{oed,ur}^{ref} / E_{oed}^{ref}$ = 1–3.

For soft clays, $E_{50}^{ref}$ can be as high as $2E_{oed}^{ref}$ (Plaxis 2022). In general, the primary loading of gravity foundations on clay is initially governed by undrained conditions. Hence, the calculation model used shall be able to estimate the undrained modulus $E_{u,50}$ from the drained $E_{50}$ when needed. The $E_{u,50}$ in undrained conditions is higher than the drained $E_{50}$ due to the higher Poisson's ratio $\nu_u \approx 0.5$.

For cases where the calculation method requires direct input of the undrained modulus, this can be estimated from undrained triaxial tests or, in the absence of laboratory data, from correlations. Figure 8-5 and Figure 8-6 illustrate the relationship between the soil modulus of clays and the undrained shear strength $s_u$.

Figure 8-5 shows a relationship between the undrained modulus $E_u$ and the undrained shear strength su as a function of the over-consolidation ratio (OCR) and plasticity index $I_p$. Figure 8-6 illustrates the relation between $G_{50}/s_u$ and the plasticity index $I_p$ of clays.

These relationships can be used for instance, when su from the Field Vane test is known. Alternatively, the $G_{max}/s_u^{DSS}$ ratio can be estimated according to Andersen (2015) if $s_u^{DSS}$, roughly corresponding to Field Vane test conditions, OCR, and plasticity index $I_p$ is known (section 4). The $G_{max}$ can then be reduced according to shear stress mobilization via the modulus reduction factor ($MRF$) presented in section 4.

Figure 8-5 Ratio $E_u/s_u$ as a function of OCR and $I_p$ (Duncan and Buchignani 1976).

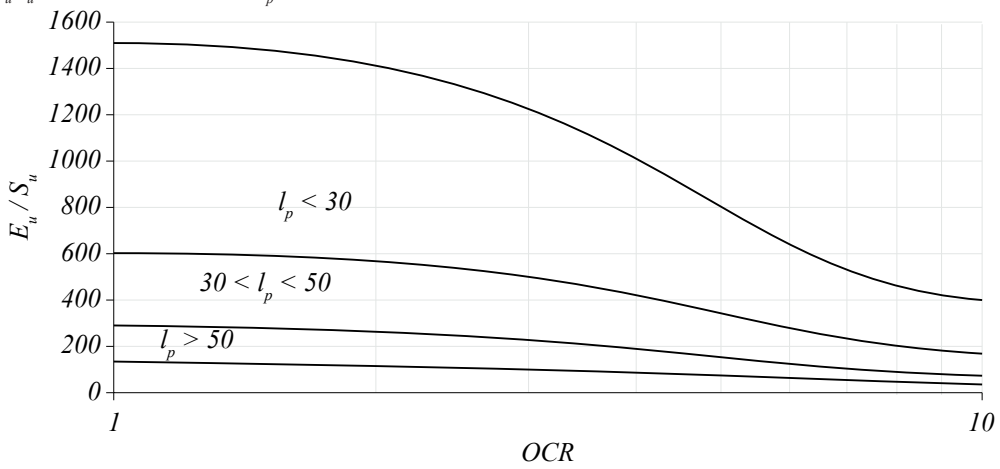

Figure 8-6 Ratio $G/s_u$ as a function of $I_p$ (Termaat et al. 1985).

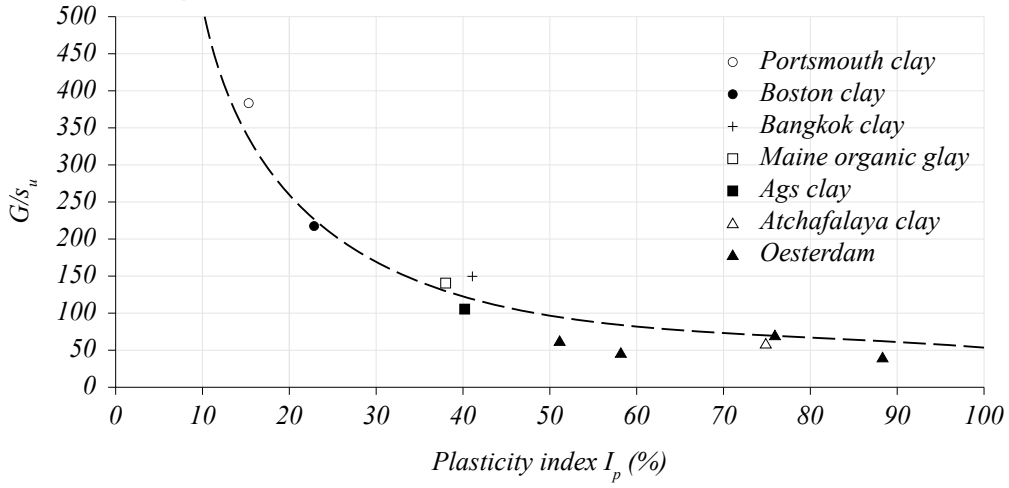


# 9. STEP-BY-STEP PROCEDURE FOR THE DETERMINATION OF $E_{50}$ AND $E_{ur}$

## 9.1. General remarks and procedure flow

As discussed in previous chapters, the determination of soil modulus can follow different paths based on the available soil data for a specific project. This chapter summarizes a step-by-step procedure to establish the drained triaxial secant Young's modulus at 50% of the maximum deviator stress $E_{50}$ and the unloading/reloading modulus $E_{ur}$ for both coarse-grained and fine-grained soils, based on the information presented in this report.

Triaxial testing on coarse-grained material is generally carried out as drained. Therefore, determining $E_{50}$ from the $q$-$\varepsilon_a$ stress-strain curve is straightforward. On the other hand, undrained triaxial testing is more common in fine-grained material. In this case, it is recommended to estimate $G_{50}$ from the shear stress $\tau = q/2$ vs shear strain $\gamma = 1.5\varepsilon_a$ curve and estimate the drained $E_{50} = 2G_{50}(1+\nu)$.

In general, the primary loading of gravity foundations on clay is initially governed by undrained conditions. Hence, the calculation should also be able to estimate the undrained modulus $E_{u,50}$ from the drained $E_{50}$. The $E_{u,50}$ in undrained conditions is higher than the drained $E_{50}$ due to the higher Poisson's ratio $\nu_u \approx 0.5$. For cases where the calculation method requires direct input of the undrained modulus, this can be estimated directly from, e.g., Figure 8-5 from OCR and $I_p$ or, alternatively, estimate $G_{50}$ from $s_u$ and $I_p$ from Figure 8-6 and calculate $E_{u,50} = 2G_{50}(1+\nu_u) \approx 3G_{50}$.

In geotechnical interpretative reports, Young's modulus is often given without information on the strain level at which it is estimated. Especially when $E$ (or $E'$) for coarse-grained soils is determined from CPT/CPTu, the correlations by Robertson and Cabal (2015) presented in chapter 7.3 are used. Young's modulus can then be considered as the modulus at 0.1% strain. Based on this, Obrzud and Truty (2018) proposed a method to estimate $E_{50}$ from $E'$ (or $E_s$, static), as a function of cohesion and friction angle of the soil, as shown in Figure 9-1.

Figure 9-1 Relationship between the $E_{50}$ and $E$ at 0.1% strain as a function of cohesion and friction angle (Obrzud and Truty 2018).

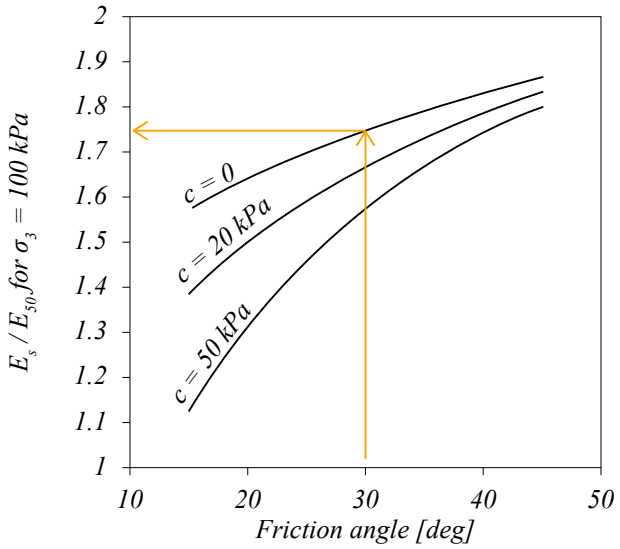


## 9.2. Determination of $E_{50}$ and $E_{ur}$

Figures 9-2 and Figure 9-3 illustrate the steps to determine $E_{50}$ and $E_{ur}$ based on the available soil data. Note that while there are "decision gates" based on which types of tests are available, engineering judgment should be applied. Different methods may often give conflicting results, and it's up to the designer to choose which estimate of modulus is the most reliable. In general, the fewer correlations and conversions are needed, the less uncertainty there is.

When using modulus reducing factor, MRF covered in Chapter 4 and mentioned in Figures 9-2 and 9-3 geo enginner shall check or understand if soils characteristic to the region confirms to stated $G_{max}/G$ relations. Evidence suggests that for specific soils (for example, highly consolidated low plasticity clays with very high $G_{max}$), given relations are not valid and may give too high $E_{50}$ values.

It should still be noted that while directly testing good quality samples can be considered the ideal method of determining soil modulus, **well-established correlations from in situ measurements should be preferred over testing of poor-quality samples.**

For fine-grained soils such as clays, good quality samples can be achieved, e.g., by using piston samplers, large diameter tube samplers, or by taking block samples (see, e.g., standard ISO 22475-1). Core drilling and other "violent" sampling methods will likely disturb the soil structure enough that laboratory testing of such samples will show a much lower modulus than what could be determined from good quality samples or in situ testing. Furthermore, good quality samples must be properly handled and stored to avoid sample disturbance.

Figure 9-2 Flow-chart for determination of drained $E_{50}$ and $E_{ur}$ for coarse-grained material.

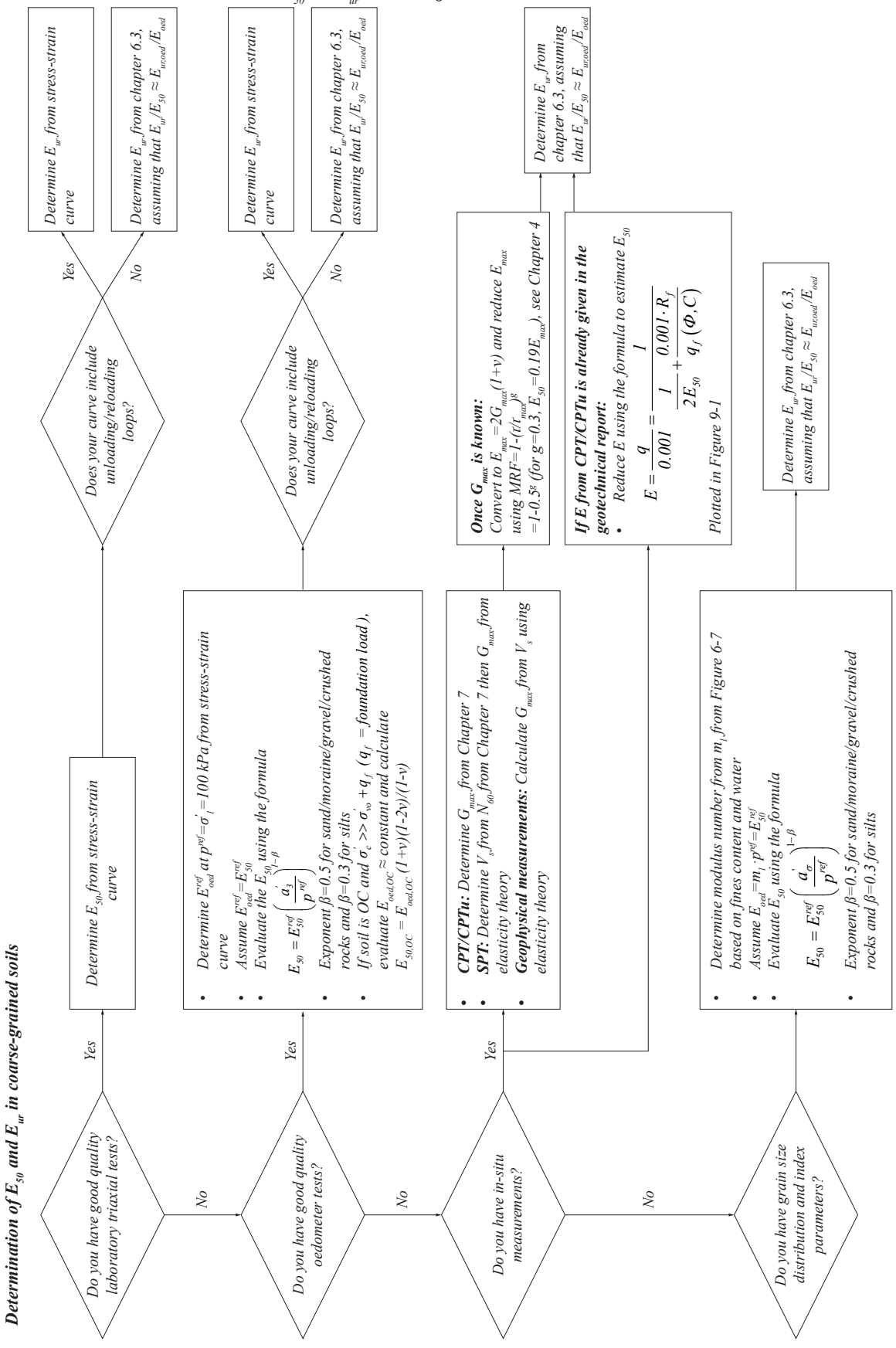

Figure 9-3 Flow-chart for determination of drained $E_{50}$ and $E_{ur}$ for fine-grained material.

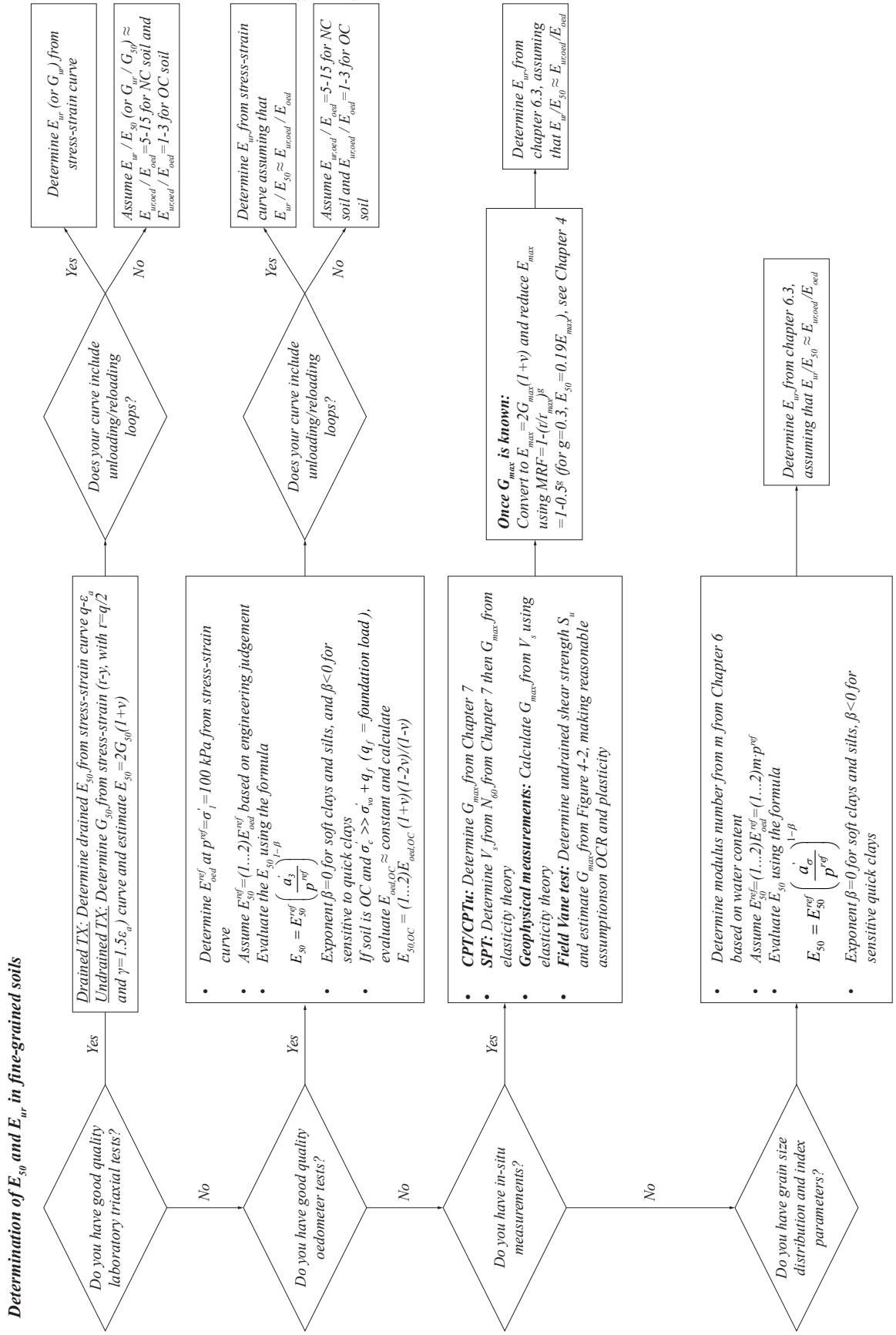

## 9.3. Applying determined modulus values to software with HS formulation

Before design calculations can be made, the stress-dependency of soil stiffness should be modeled in the design software accordingly. Any modulus value determined from laboratory or in situ data is associated with a stress level where it has been determined (i.e., the in situ stress state or the stress state to which the soil sample has been consolidated). The determined modulus value must be converted to a reference modulus value at a reference stress level.

A typical conversion that often needs to be made is to convert measured (or otherwise determined) modulus $E$ at a given stress state to the reference value $E'_{ref}$ at the reference stress $p^{ref}$ = 100 kPa.

We have the general relationship (here, $E$ is presented as a function of vertical stress, as is typically done in relation to oedometer testing):

$$E = E\left(\sigma'_v\right) = E^{ref}\left(\frac{\sigma'_v}{p^{ref}}\right)^{1-\beta}$$

<–>

$$E^{ref}\frac{E}{\left(\frac{\sigma'_v}{p^{ref}}\right)^{1-\beta}}$$

Depending on the calculation software, this relationship may also be given as a function of effective mean stress $p'$ or minor principal stress $\sigma'_3$. The user should be aware of which relationship is used in the given context.

One significant case is software that uses the Hardening Soil formulation for stress-dependent soil stiffness ($E_{50}$ or $E_{ur}$, see e.g. Obrzud & Truty 2018):

$$E = E\left(\sigma'_3\right) = E^{ref}\left(\frac{\sigma^*_3 + c\cdot\cot\left(\varphi\right)}{\sigma^{ref} + c\cdot\cot\left(\varphi\right)}\right)^{m}$$

where :
$E$ is either $E_{50}$ or $E_{ur}$
$E_{ref}$ is the corresponding reference modulus at the given reference stress
$\sigma^*_3$ is $max(\sigma'_3; 10\ kPa)$
$\sigma^{ref}$ is the minor stress where the stiffness $E$ is determined.
$m$ is the stress exponent (equivalent to $1\text{-}\beta$ in the general formulation – **not** the tangent modulus method modulus number!)

Note that Obrzud & Truty (2018) are not quite clear in their notation between effective and total stresses, but effective stresses are implied as modulus depends on effective stresses.

The Hardening Soil formulation allows the reference stress value can be chosen freely. Therefore, if $E_{50}$ has been determined, for example, from a triaxial test, the cell pressure $\sigma'_3$ can be input as the reference stress $\sigma^{ref}$, and the reference modulus is directly the modulus value determined from the test.

If the $E_{50}$ value is determined based on in situ testing or unconsolidated triaxial testing, the reference stress should correspond to the stress at the depth where the test is done or where the sample is taken. The vertical stress at a given depth can generally (assuming horizontal soil layers) be calculated as:

$$\sigma_v^{'} = \sigma_v - u = \sum\left(h_i \cdot \gamma_i\right) - u$$

where:
$h_i$ and $\gamma_i$ are the thickness and total unit weight of a given soil layer above the given depth
$u$ is the pore pressure at the given depth.

For conversion between $\sigma_v^{'}$ and $\sigma_3^{'}$, the following Equation may be used (while assuming that the minor principal stress is the horizontal stress:

$$\sigma_3^{'} = \sigma_h^{'} = k0 \cdot \sigma_v^{'}$$

As an alternative to using the test stress as the reference stress, one can express the $E$ value at the "standard level" of 100 kPa. The conversion to reference stress can then be made by:

$$E^{ref} = \frac{E}{\left(\frac{\sigma_3^{*} + c \cdot \cot\left(\varphi\right)}{\sigma^{ref} + c \cdot \cot\left(\varphi\right)}\right)^{m}}$$

where:
$E$ is the determined modulus from the test
$\sigma_3^{*}$ is the effective minor principal stress for the test
$\sigma^{ref}$ is 100 kPa

For more detailed discussion of the Hardening Soil stiffness formulation, see e.g. Obrzud & Truty (2018) Chapter 2.

### Example, test result to Hardening Soil parameters:

For a sand ($\varphi$' = 30°, $c$' = 0.1 kPa, $m$ = 0.5, $K0$ = 0.5), $E_{50}$ has been determined to be $E_{50}$ = 50 MPa at an in situ stress state $\sigma_v^{'}$ = 70 kPa. Give the corresponding Hardening Soil input parameters $\sigma^{ref}$ and $E_{50}^{ref}$:

a) As a function of $\sigma_3^{'}$, with test stress level as the reference stress
b) As a function of $\sigma_3$, with reference stress 100 kPa
c) As a function of $p'$, with test stress level as the reference stress
d) As a function of $p'$, with reference stress 100 kPa

**a)** As a function of $\sigma_3^{'}$, with test stress level as the reference stress

$$\sigma^{ref} = \sigma_3^{*} = \sigma_h^{'} = K0 \cdot \sigma_v^{'} = 0.5 \cdot 70\ kPa = 35\ kPa$$

$$E_{50}^{ref} = E_{50} = 50\ MPa$$

**b)** As a function of $\sigma_3^{'}$, with reference stress 100 kPa

$$\sigma^{ref} = 100\ kPa$$

$$E_{50}^{ref} \frac{E_{50}}{\left(\frac{\sigma_3^{*} + c \cdot \cot\left(\varphi\right)}{\sigma^{ref} + c \cdot \cot\left(\varphi\right)}\right)^{m}} = \frac{50\ MPa}{\left(\frac{35\ kPa + 0.1\ kPa \cdot \cot\left(30°\right)}{100\ kPa + 0.1\ kPa \cdot \cot\left(30°\right)}\right)^{m}} = 84.4\ MPa$$

**c)** As a function of $p'$, with test stress level as the reference stress

$$\sigma^{ref} = p' = \frac{\sigma_v' \left(1+2+K0\right)}{3} = \frac{70kPa\left(1+2+0.5\right)}{3} = 46.7\ kPa$$

$$E_{50}^{ref} = E_{50} = 50\ MPa$$

**d)** As a function of $p'$, with reference stress 100 kPa

$$\sigma^{ref} = 100\ kPa$$

$$E_{50}^{ref} \frac{E_{50}}{\left(\frac{p^* + c \cdot cot\left(\varphi\right)}{\sigma^{ref} + c \cdot cot\left(\varphi\right)}\right)^m} = \frac{50\ MPa}{\left(\frac{46.7\ kPa + 0.1\ kPa \cdot cot\left(30°\right)}{100\ kPa + 0.1\ kPa \cdot cot\left(30°\right)}\right)^m} = 73.1\ MPa$$

# 10. SUMMARY AND CONCLUSIONS

The report has presented a comprehensive study on soil modulus for a wide range of soil types for the design and analysis of onshore wind turbine foundations. As reported, soil stress-strain behavior is non-linear. Consequently, the determination of a soil modulus is not a straightforward process. Soil modulus is not constant and is affected by several factors, including state factors (particle density, water content, stress history, cementation) and loading factors (stresses and confinement, strain level, rate effects, number of cycles, drainage, intermolecular and surface forces).

An appropriate soil modulus characterization would require an extensive set of laboratory and in-situ tests. In laboratory tests can be more directly measured modulus values needed for soil modeling, but quite often, laboratory samples can be disturbed and do not precisely represent soil conditions in-situ. However, in-situ tests usually do not measure directly needed modulus, but other parameters such as cone resistance and then using correlation can be obtained needed values. The use of correlation makes in-situ less accurate, but in-situ tests usually better represent the actual soil state in nature (soil is not disturbed). Triaxial and oedometer tests provide a good background to determine drained primary loading secant modulus ($E_{50}$), secant unloading/reloading ($E_{ur}$) and tangent constrained ($E_{oed}$) modulus. Bender element or resonant column tests are ideal for studying the small-strain tangent shear modulus $G_{max}$. However, these tests are too often limited or unavailable, especially in small-sized projects. In-situ tests can be used to estimate soil modulus based on literature correlations in the absence of site-specific laboratory tests. Among these, the cone penetration test (CPT or CPTu) is considered the most reliable. Tests such as standard penetration test (SPT) are characterized by larger uncertainty.

Weight-sounding (painokairaus) or dynamic cone penetration testing (puristinheijari), which are widely used in Finland do not provide any direct information on soil parameters. Nevertheless, national geotechnical design guidelines (NCCI 7 by Liikennevirasto, 2017) provide guidance for selecting strength and stiffness parameters of coarse-grained soils based on the results of such tests. The NCCI 7 data is based on studies done in Finland from the 1960's onwards, which have been part of the established engineering practice from at least the 1990's onwards when they were incorporated in official bridge design manuals and later to higher level guidelines. They are often referred to even in projects that are not governed by NCCI 7 (i.e. projects not related to traffic infrastructure). As such, their use in Finland can be considered safe in terms of established practice. They do not have the same status outside of Finland but may still be carefully used as background reference material. Additional, locally established references may be required.

The report further summarized correlations to establish soil modulus for different soil types in the absence of laboratory data for both coarse-grained and fine-grained soils. These are based on basic soil index properties. These correlations shall be only used for a preliminary estimate of foundation performance and validated by means of laboratory and/or in-situ tests during subsequent design phases.

A final chapter illustrates a step-by-step procedure to determine $E_{50}$ and $E_{ur}$ based on the available soil investigation data for both coarse-grained and fine-grained soils. The aim is to provide a tool to guide geotechnical designers through the contents of this report when establishing design parameters.

# 11. REFERENCES


Allen, F. A., F. E. Richart Jr, and R. D. Woods. 1980. Fluid wave propagation in saturated and nearly saturated sands, J. Geotech. Eng. ASCE 106, 235–254.

Alpan, I. (1970). The geotechnical properties of soils. Earth-Science Reviews, 6:5–49.

Andersen, K.H., 2015. Cyclic soil parameters for offshore foundation design. 3rd ISSMGE McClelland Lecture. Frontiers in Offshore Geotechnics III, ISFOG'2015, Meyer (Ed). Taylor & Francis Group, London, ISBN: 978-1-138-02848-7. Proc., 5-82. Rev. version in: http://www.issmge.org/committees/technical-committees/applications/offshore and click on "Additional Information".

Andersen, K. H., & Schjetne, K. (2013). Database of friction angles of sand and consolidation characteristics of sand, silt, and clay. Journal of Geotechnical and Geoenvironmental Engineering, 139(7), 1140-1155.

Benz, T. (2007). Small-strain stiffness of soils and its numerical consequences. Phd, Universitat Sttutgart.

Briaud, J. L. 2013. Geotechnical engineering: unsaturated and saturated soils. John Wiley & Sons.

Casey, B., J.T. Germaine, N.O. Abdulhadi, N.S. Kontopoulos, and C.A. Jones. 2016. Undrained Young's Modulus of Fine-Grained Soils. Journal of Geotechnical & Geoenvironmental Engineering, Vol. 142, No. 2, 04015070.

Darendeli, M.B. 2001. "Development of a New Family of Normalized Modulus Reduction and Material Damping Curves." Ph.D. thesis, The University of Texas, Austin.

Di Buò, B. 2020. Evaluation of the Preconsolidation Stress and Deformation Characteristics of Finnish Clays based on Piezocone Testing. PhD Thesis, Tampere University, Tampere, Finland. ISBN 978-952-031468-2

Di Buò, B., Selänpää, J., Länsivaara, T., and D'Ignazio, M. 2018. Evaluation of existing CPTu-based correlations for the deformation properties of Finnish soft clays. In Cone Penetration Testing 2018. pp. 185–191. CRC Press.

D'Ignazio, M. 2016. Undrained shear strength of Finnish clays for stability analyses of embankments. PhD thesis, Department of Civil Engineering, Tampere University of Technology, Tampere, Finland.

D'Ignazio, M. 2022. Personal communication.

Duncan, J.M. & Chang, C. Y, 1970. Non-linear Analysis of Stress And Strain in Soil. ASCE Journal of the Soil Mechanic And Foundation. Div. Vol. 96, pp. 1629-1653.

Duncan, J. M., & Buchignani, A. L. 1976. An Engineering Manual for Settlement Studies: By JM Duncan and AL Buchignani. Department of Civil Engineering, University of California.

Fahey, M. and Carter, J.P. 1993. A finite element study of the pressuremeter in sand using a non-linear elastic plastic model. Canadian Geotechnical Journal, 30(2): 348-362.

Helenelund, K.V. 1964. Moreenimaalajien kantavuusominaisuuksista. VTT, sarja III – rakennus 79, Helsinki

Helenelund, K.V. 1966. Kitkamaalajien kantavuusominaisuuksista. VTT, sarja III – rakennus 97, Helsinki

Janbu N. 1963. Soil Compressibility as Determined by oedometer and Triaxial Tests. Proceedings 4th European Conference on Soil Mechanics and foundation Engineering. Wiesbaden 1. 19-25.

Janbu, N. 1985. Soil models in offshore engineering. Géotechnique, 35(3): 241-281.

Janbu, N. 1998. Sediment deformations, NTNU Bulletin 35. Trondheim, Norway.

Jefferies, M.G., and Davies, M.P. 1993. Use of CPTU to estimate equivalent SPT N60. Geotech-nical Testing Journal, ASTM, 16(4): 458-468.

Karlsrud, K., and Hernandez-Martinez, F.G. 2013. Strength and deformation properties of Norwegian clays from laboratory tests on high-quality block samples. Canadian Geotechnical Journal, 50(12): 1273-1293.

Kondner, R.L., 1963. A Hyperbolic Stress Strain Formulation for sands. 2. Pan. Am. ICOSFE Brazil, Vol. 1,pp. 289-324.

Kulhawy, F.H. and Mayne, P.W. 1990. Manual on Estimating Soil Properties for Foundation Design. Report EL-6800, Electric Power Research Institute, Palo Alto, California.

Liikennevirasto (2017). Eurokoodin soveltamisohje – Geotekninen suunnittelu – NCCI 7. Siltojen ja pohjarakenteiden suunnitteluohjeet 21.4.2017. Liikenneviraston ohjeita 13/2017.

Lunne, T., Robertson, P.K., and Powell, J.J.M. 1997. Cone penetration testing in geotechnical practice. Blackie Academic, EF Spon/ Routledge Publ., New York, 1997, 312 pp.

Länsivaara, T. 1999. A study of the mechanical behavior of soft clay. PhD Dissertation, Norwegian University of Science and Technology, Norway.

Mansikkamäki, J. 2015. Effective stress finite element stability analysis of an old railway embankment on soft clay. PhD thesis, Department of Civil Engineering, Tampere University of Technology, Tampere, Finland.

Mansikkamäki, J. 2022. Computational Geotechnics II course, lectures slides. Tampere University, Finland.

Mayne, P.W., 2005. Integrated Ground Behavior: In-Situ and Lab Tests. In Proceedings of the International Symposium on Deformation Characteristics of Geomaterials, Lyon, France, 22-24 September 2005. Taylor & Francis, London, pp. 155-177.

Mayne, P.W. 2007. In-situ test calibrations for evaluating soil parameters. In Characterization & Engineering Properties of Natural Soils, Vol. 3 (Proc. Singapore 2006), Taylor & Francis Group, London, pp. 1602–1652.

Mayne, P.W. 2007. NCHRP Synthesis 368 on Cone Penetration Test. Transportation Research Board, National Academies Press, Washington, DC.

Mayne, P. and Rix, G. 1993. Gmax-qc relationships for clays. Geotechnical Testing Journal, 16(1):54–60.

Mitchell, J.K., Guzikowski, F. and Villet, W.C.B. 1978. The Measurement of Soil Properties In-Situ, Report prepared for US Department of Energy Contract W-7405-ENG-48, Lawrence Berkeley Laboratory, University of California, Berkeley, CA, 94720.

Obrzud R.F, and Truty, A. 2018. The Hardening Soil model – a practical guidebook. Technical report Z_Soil.PC 100701, Zace Services Ltd, Lausanne, Edition 2018.

Ohta, H. and Goto, N. (1976). Estimation of s-wave velocity in terms of characteristic indices of soil (in Japanese). Buturi-tansa, 29:251–261

PLAXIS 2022. Bentley Plaxis user's manual

Rix, G. J., & Stokoe, K. H. (1991). Correlation of initial tangent modulus and cone resistance, Calibration Chamber Testing.

Rix, G.J., Mayne, P.W., Bachus, R.C., et al. 2019. NCHRP Manual on Subsurface Investigation, Web Document 258, DOI: 10.17226/25379.

Robertson, P.K. 1990. Soil classification using the cone penetration test. Canadian Geotechnical Journal, 27(1), 151-158.

Robertson, P. K. 2009. Interpretation of cone penetration tests - a unified approach. Canadian geotechnical journal, 46(11): 1337-1355.

Robertson, P. and Campanella, R. (1983). Interpretation of cone penetration tests. part I: Sand. Can Geotech J, 20(4):718–33.

Robertson. P.K., Campanella, R.G., Gillespie, D., and Greig, J. 1986. Use of Piezometer Cone data. In-Situ'86: Use of In Situ Tests in Geotechnical Engineering, Blacksburg, Va., 23-25 June 1986. Geotechnical Special Publication No. 6, ASCE, New York, pp. 1263-1280.

Robertson, P. K., & Cabal, K. L. (2015). Guide to cone penetration testing for geotechnical engineering. Gregg Drilling & Testing, Inc, 6.

Schanz, T. 1998. Zur modellierung des mechanishen verhaltens von reibungsmaterialen Habilitation. Stuttgard University.

Skempton, A.W. 1986. Standard Penetration Test Procedures and Effects in Sands of Overbur-den Pressure, Relative Density, Particle Size, Ageing, and Over Consolidation. Geotechnique, Vol. 36, No. 3, pp. 425–447.

Tammirinne, M 1969. Kitkamaalajien rakenne ja kokoonpuristuvuus. VTT, sarja III – rakennus 136, Helsinki

Termaat, R.J., Vermeer, P.A., Vergeer, C.J.H. 1985. Failure by large plastic deformations. In Proceedings of the 11th International Conference on Soil Mechanics and Foundation Engineering, San Francisco, 12-16 Aug

Vardanega, P.J., and M.D. Bolton. 2013. “Stiffness of Clays and Silts: Normalizing Shear Modulus and Shear Strain.” Journal of Geotechnical & Geoenvironmental Engineering, 10.1061/(ASCE)GT.1943-5606.0000887: 1575–1589.

Valkeisenmäki, A. 1973. Rakeisuuden vaikutus hiekan ja soran painumis- ja tiiveysominaisuuksiin. Otaniemi, VTT, Geotekniikan laboratorio, tiedonanto 10.

Vucetic, M., and R. Dobry. 1991. "Effect of Soil Plasticity on Cyclic Response." Journal of Geotechnical Engineering, Vol. 117, No. 1, pp. 89–107.

Youd, T.L., M. Idriss, R.D. Andrus, I. Arango, G. Castro, J.T. Christian, R. Dobry, W.D.L. Finn, L.F. Harder, Jr., M.E. Hynes, K. Ishihara, J.P. Koester, S.S.C. Liao, W.F. Marcuson, III, G.R. Martin, J.K. Mitchell, Y. Moriwaki, M.S. Power, P.K. Robertson, R.B. Seed, and K.H. Stokoe, II. 2001. "Liquefaction Resistance of Soils: Summary Report from the 1996 NCEER and 1998 NCEER/NSF Workshops on Evaluation of Liquefaction Resistance of Soils." Journal of Geotech-nical and Geoevironmental Engineering, Vol. 127, No. 10, pp. 817–833.

## EXPERT ADVICE LOCALLY AVAILABLE

Peikko's operations are based on localized and reliable customer service, excellence in R&D and manufacturing. This includes good co-operation with customers, other stakeholders, and within society. Our overall aim is to consistently deliver high quality and to work in an environmentally aware manner.

**www.peikko.com**

# A faster, safer, and more efficient way to design and build

Peikko supplies slim floor structures and connection technology for precast and cast-in-situ applications. Peikko's innovative solutions make your construction process more efficient.